6. Physics of W and Z bosons

6.1 W and Z Bosons in the Glashow-Salam-Weinberg theory

6.2 Summary of precision tests at LEP

6.3 W and Z boson production in hadron colliders

6.4 Test of QCD in W/Z (+jet) production

6.5 W mass measurement

Weak Isospin and Hypercharge Quantum

Lepton	T	T^3	Q	Y
ν_e	$\frac{1}{2}$	$\frac{1}{2}$	0	-1
e^-_L	$\frac{1}{2}$	$-\frac{1}{2}$	-1	-1
e^-_R	0	0	-1	-2

Numbers of Leptons and Quarks

Quark	T	T^3	Q	Y
u_L	$\frac{1}{2}$	$\frac{1}{2}$	$\frac{2}{3}$	$\frac{1}{3}$
d_L	$\frac{1}{2}$	$-\frac{1}{2}$	$-\frac{1}{3}$	$\frac{1}{3}$
u_R	0	0	$\frac{2}{3}$	$\frac{4}{3}$
d_R	0	0	$-\frac{1}{3}$	$-\frac{2}{3}$

W and Z vertex factors

$$-i\frac{g}{\sqrt{2}}\left(\bar{\chi}_L\gamma^\mu\tau_+\chi_L\right)W_\mu^+$$
$$= -i\frac{g}{\sqrt{2}}\left(\bar{\nu}_L\gamma^\mu e_L\right)W_\mu^+$$

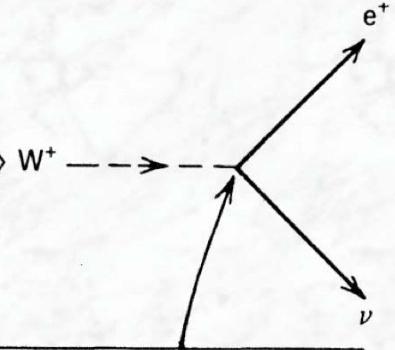

$$-i\frac{g}{\sqrt{2}}\gamma^\mu\tfrac{1}{2}\left(1-\gamma^5\right)$$

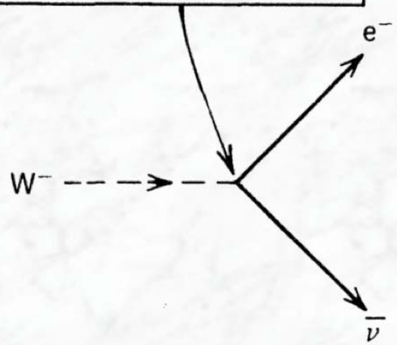

$$-i\frac{g}{\sqrt{2}}\left(\bar{\chi}_L\gamma^\mu\tau_-\chi_L\right)W_\mu^-$$
$$= -i\frac{g}{\sqrt{2}}\left(\bar{e}_L\gamma^\mu\nu_L\right)W_\mu^-$$

⇨ 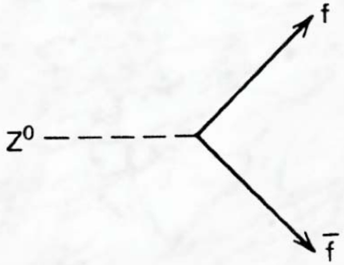

$$-i\frac{g}{\cos\theta_W}\gamma^\mu\tfrac{1}{2}\left(c_V^f-c_A^f\gamma^5\right).$$

The Z → ff vertex factors in the Standard Model

(sin^2 θ_W is assumed to be 0.234)

$\mathbf{f}$	$\mathbf{Q}_f$	$\mathbf{c}_A^f$	$\mathbf{c}_V^f$
$\nu_e, \nu_\mu, \ldots$	0	$\frac{1}{2}$	$\frac{1}{2}$
$e \quad , \mu \quad , \ldots$	-1	$-\frac{1}{2}$	$-\frac{1}{2} + 2\sin^2\theta_W \quad 0.03$
$u, c, \ldots$	$\frac{2}{3}$	$\frac{1}{2}$	$\frac{1}{2} \quad \frac{4}{3}\sin^2\theta_W \quad 0.19$
$d, s, \ldots$	$-\frac{1}{3}$	$-\frac{1}{2}$	$-\frac{1}{2} + \frac{2}{3}\sin^2\theta_W \quad 0.34$

6.2 Summary of electroweak precision tests at LEP

- Results of 30 years of experimental and theoretical progress
- The electroweak theory is tested at the level of 10^{-4}

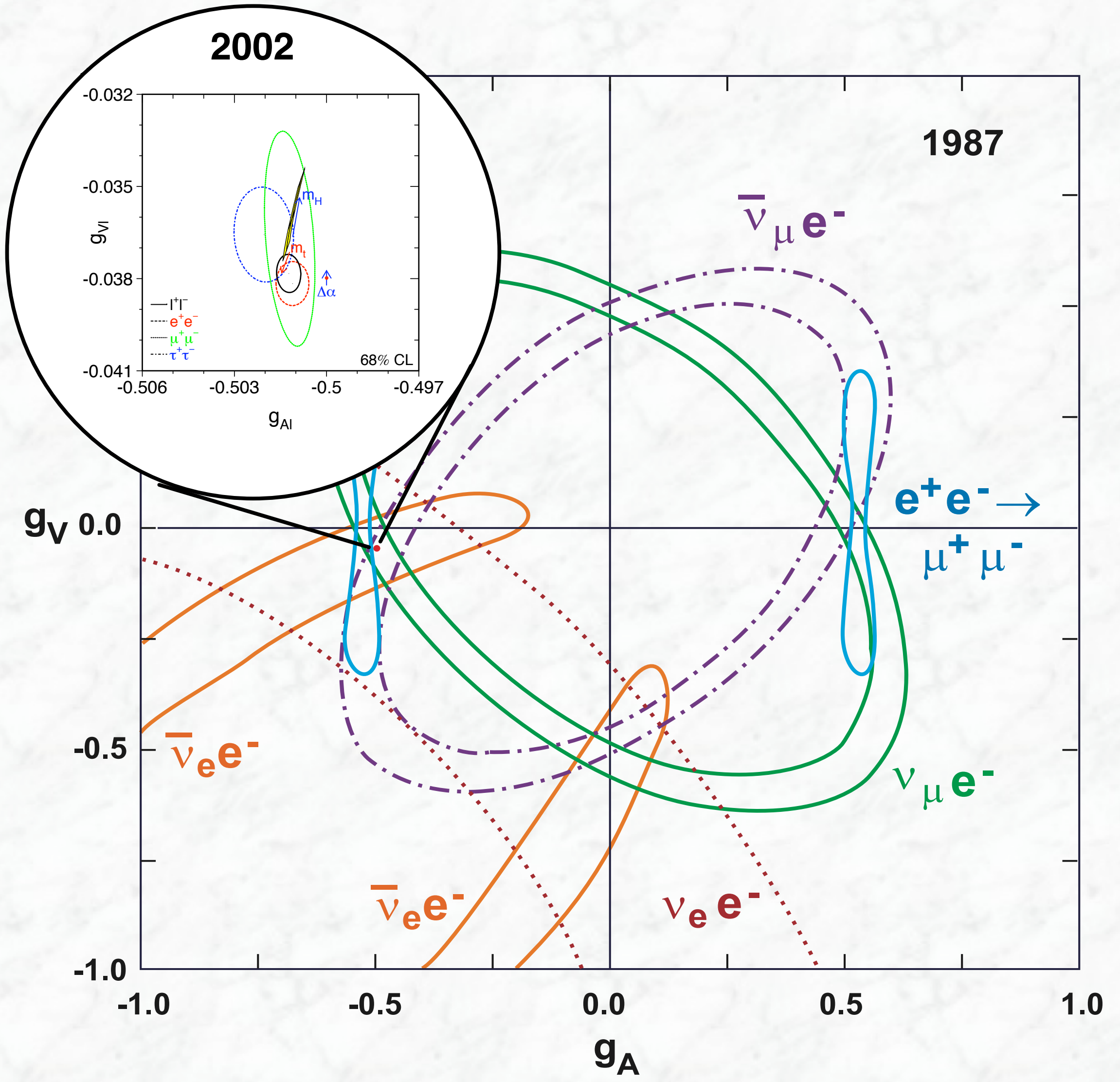


LEP am CERN / Genf
ALEPH
L3
LEP / LHC
SPS
OPAL
DELPHI
e⁺e⁻-Beschleuniger, 27 km Umfang
Schwerpunktsenergie: LEP-I (1989-1995) 91 GeV
LEP-II (1996-2000) → 208 GeV
4 Experimente: ALEPH, DELPHI, L3, OPAL

Cross sections for W and Z boson production

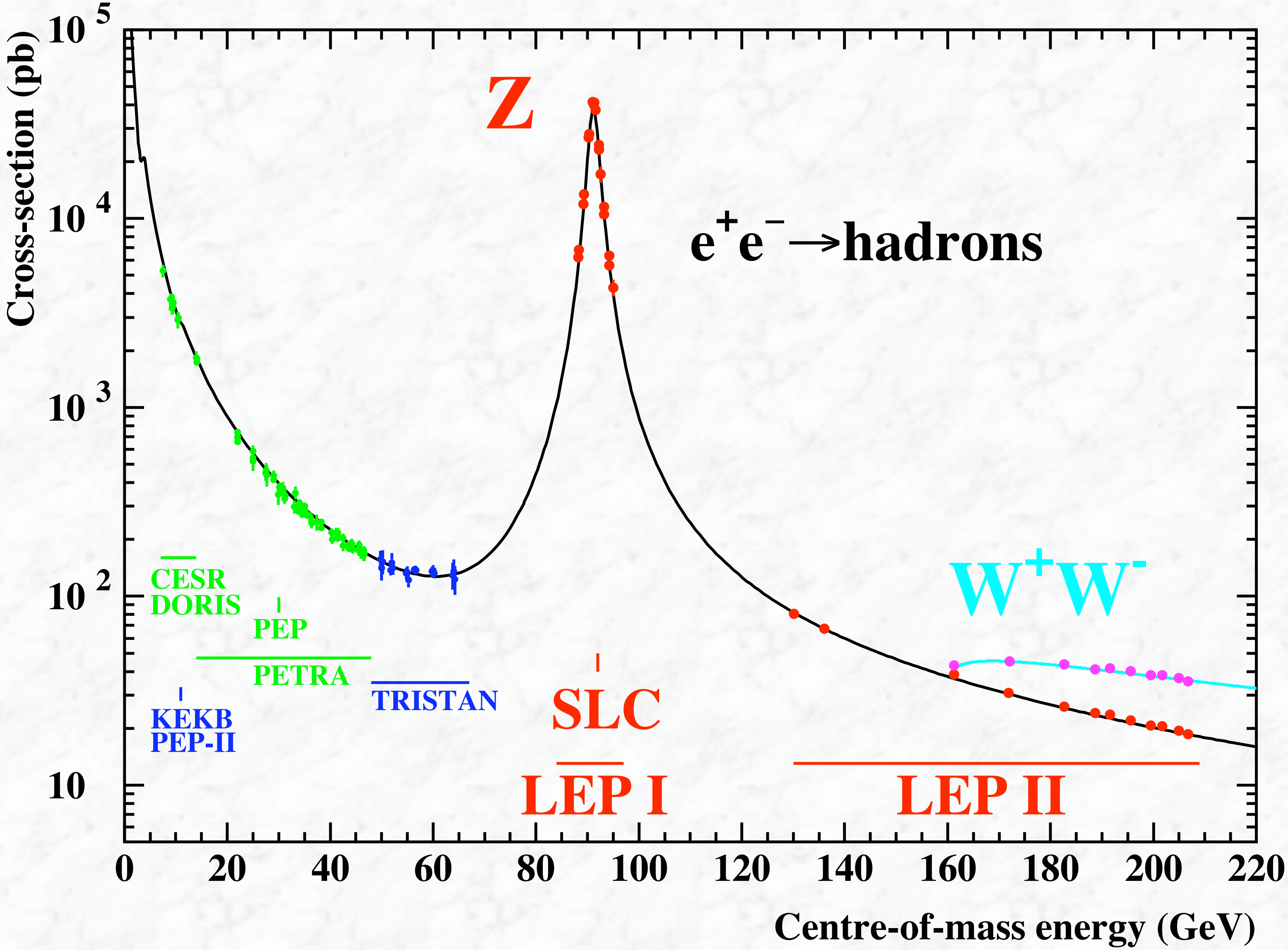

Precision tests of the Z sector

Tests of the W sector

Cross section for $e^+e^- \rightarrow \mu^+\mu^-$ at LEP I

$$\frac{d\sigma}{d\cos\theta} = \frac{\pi\alpha^2}{2s}\left[F_\gamma(\cos\theta) + F_{\gamma Z}(\cos\theta)\frac{s(s-M_Z^2)}{(s-M_Z^2)^2+M_Z^2\Gamma_Z^2} + F_Z(\cos\theta)\frac{s^2}{(s-M_Z^2)^2+M_Z^2\Gamma_Z^2}\right]$$

γ — γ/Z interference — Z

γ/Z interference: vanishes at $\sqrt{s} \approx M_Z$

$$F_\gamma(\cos\theta) = Q_e^2 Q_\mu^2(1+\cos^2\theta) = (1+\cos^2\theta)$$

$$F_{\gamma Z}(\cos\theta) = \frac{Q_e Q_\mu}{4\sin^2\theta_W\cos^2\theta_W}\left[2g_V^e g_V^\mu(1+\cos^2\theta) + 4g_A^e g_A^\mu\cos\theta\right]$$

$$F_Z(\cos\theta) = \frac{1}{16\sin^4\theta_W\cos^4\theta_W}\left[(g_V^{e^2}+g_A^{e^2})(g_V^{\mu^2}+g_A^{\mu^2})(1+\cos^2\theta) + 8g_V^e g_A^e g_V^\mu g_A^\mu\cos\theta\right]$$

$\alpha=\alpha(m_Z)$: running el.magnetic coupling [$\alpha(M_Z) = \alpha/(1-\Delta\alpha)$ mit $\Delta\alpha\approx 0.06$]

$g_V, g_A = c_V, c_A$: effective coupling constants (vector and axial vector)

Cross section for $e^+e^- \rightarrow f\bar{f}$ at LEP I

$$\frac{d\sigma}{d\cos\theta} = \frac{\pi\alpha^2}{2s}\left[F_\gamma(\cos\theta) + F_{\gamma Z}(\cos\theta)\frac{s(s-M_Z^2)}{(s-M_Z^2)^2+M_Z^2\Gamma_Z^2} + F_Z(\cos\theta)\frac{s^2}{(s-M_Z^2)^2+M_Z^2\Gamma_Z^2}\right]$$

γ

γ/Z interference

Z

vanishes at $\sqrt{s} \approx M_Z$

x N_C^f
number of colour degrees of freedom for für fermion f

x $(1+\delta_{QCD})$
QCD correction term

$$F_\gamma(\cos\theta) = Q_e^2 Q_f^2 (1+\cos^2\theta) = (1+\cos^2\theta)$$

$$F_{\gamma Z}(\cos\theta) = \frac{Q_e Q_f}{4\sin^2\theta_W \cos^2\theta_W}\left[2 g_V^e g_V^\mu (1+\cos^2\theta) + 4 g_A^e g_A^f \cos\theta\right]$$

$$F_Z(\cos\theta) = \frac{1}{16\sin^4\theta_W \cos^4\theta_W}\left[({g_V^e}^2 + {g_A^e}^2)({g_V^f}^2 + {g_A^f}^2)(1+\cos^2\theta) + 8 g_V^e g_A^e g_V^f g_A^f \cos\theta\right]$$

Cross section for $e^+e^- \rightarrow f\bar{f}$ on resonance ($\sqrt{s} = m_Z$)

- On resonance, $\sqrt{s} = m_Z$:
  - γ^*/Z interference terms vanishes
  - γ term contributes ~1%
  - Z contribution dominates !

- Contribution of the γ^*/Z interference term at $s = (M_Z - 3\text{ GeV})^2$: ~0.2%

Total cross section for $e^+e^- \rightarrow \mu^+\mu^-$ (integration over cos θ)

$$\sigma_{\text{tot}} \approx \sigma_Z = \frac{4\pi}{3s}\frac{\alpha^2}{16\sin^4\theta_W\cos^4\theta_W}\cdot[(g_V^e)^2+(g_A^e)^2][(g_V^\mu)^2+(g_A^\mu)^2]\cdot\frac{s^2}{(s-M_Z^2)^2+(M_Z\Gamma_Z)^2}$$

$$\sigma_Z(\sqrt{s}=M_Z) = \frac{12\pi}{M_Z^2}\frac{\Gamma_e\Gamma_\mu}{\Gamma_Z^2}$$

Peak cross section

$$\Gamma_f = \frac{\alpha M_Z}{12\sin^2\theta_W\cos^2\theta_W}\cdot[(g_V^f)^2+(g_A^f)^2]$$

Partial width

$$\Gamma_Z = \sum_i \Gamma_i$$

Total width

From the energy dependence of the total cross section (for various fermions f) the parameters

M_Z, Γ_Z, Γ_f

can be determined.

Measurement of the Z line-shape

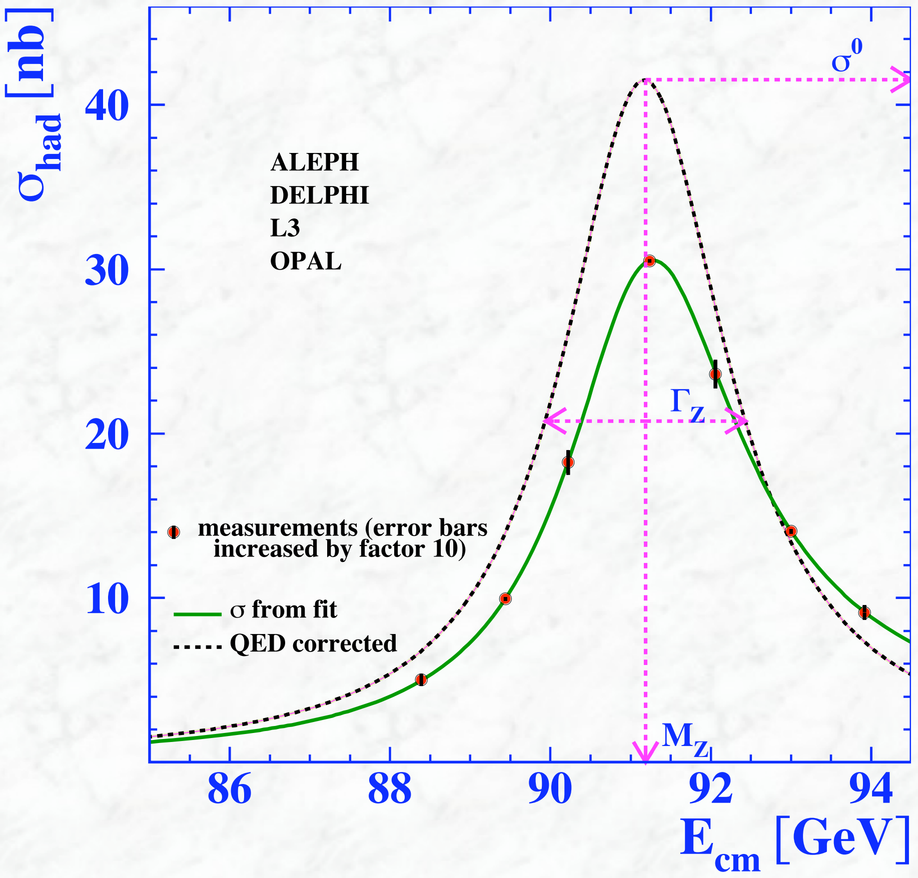

Line shape (resonance curve):

$$\sigma(s) = 12\pi \frac{\Gamma_e \Gamma_\mu}{M_Z^2} \cdot \frac{s}{(s-M_Z^2)^2 + M_Z^2 \Gamma_Z^2}$$

Peak: $\sigma_0 = \frac{12\pi}{M_Z^2} \frac{\Gamma_e \Gamma_\mu}{\Gamma_Z^2}$

- Position of maximum $\rightarrow$ M_Z
- Full width at half maximum $\rightarrow$ Γ_Z
- Peak cross section σ_0 $\rightarrow$ $\Gamma_e \Gamma_\mu$

Radiative corrections (photon radiation) important

with ISR (initial state radiation)

without ISR

Measurement of the Z line-shape (cont.)

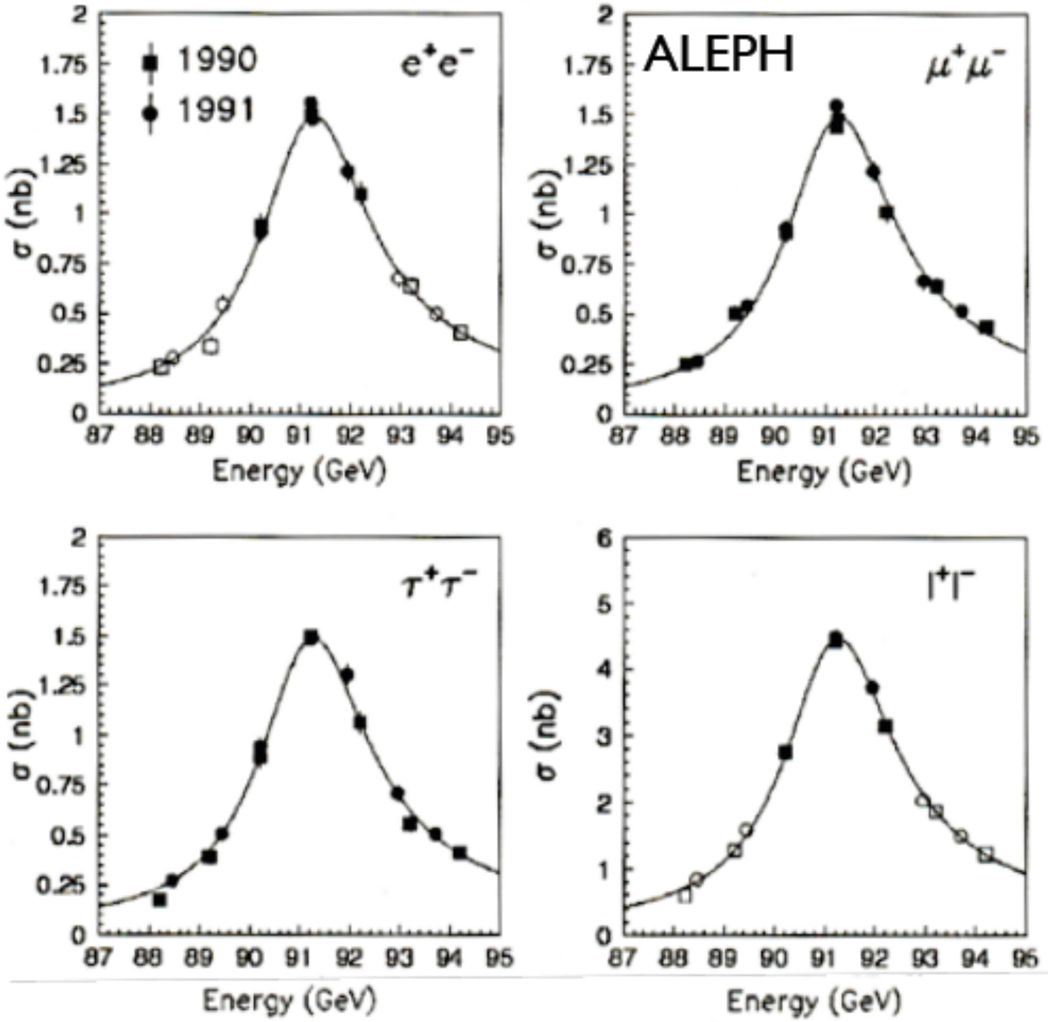

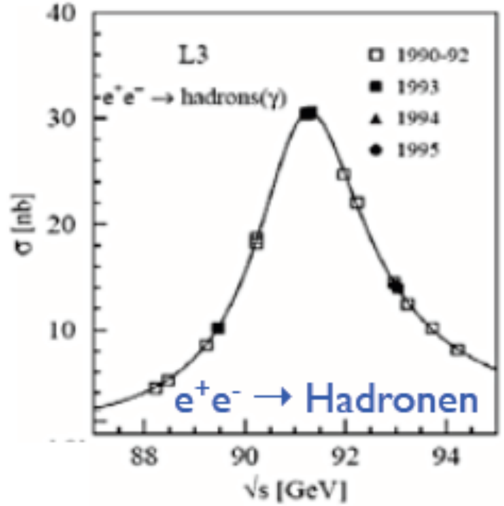

Quark-Flavor i.a. nicht exp. trennbar
(Ausnahme: c,b → Lebendsdauer)
⇒ had. Breite: $\Gamma_{had} = \Gamma_u + \Gamma_d + \Gamma_s + \Gamma_c + \Gamma_b$

Messe Verhältnisse der Pol-WQ:

$$R_l^0 \equiv \frac{\Gamma_{had}}{\Gamma_{ll}} \qquad l = e, \mu, \tau$$

$$R_q^0 \equiv \frac{\Gamma_{qq}}{\Gamma_{had}} \qquad q = b, c$$

- Keine Unterschiede für verschiedene Leptonarten ⇒ Leptonuniversalität
- Form der Resonanzenkurve für alle Endzustände gleich (gleicher Propagator!)

Results on Z line-shape parameters

$M_Z = 91.1876 \pm 0.0021$ GeV   23 ppm (*)

$\Gamma_Z = 2.4952 \pm 0.0023$ GeV
$\Gamma_{had} = 1.7458 \pm 0.0027$ GeV
$\Gamma_e = 0.08392 \pm 0.00012$ GeV
$\Gamma_\mu = 0.08399 \pm 0.00018$ GeV
$\Gamma_\tau = 0.08408 \pm 0.00022$ GeV

3 lepton flavours treated independently

Test of lepton universality

$\Gamma_Z = 2.4952 \pm 0.0023$ GeV
$\Gamma_{had} = 1.7444 \pm 0.0022$ GeV
$\Gamma_e = 0.083985 \pm 0.000086$ GeV

lepton universality assumed:
$\Gamma_e=\Gamma_\mu=\Gamma_\tau$

*) Uncertainty on LEP energy measurement: ± 1.7 MeV (19 ppm)

Number of neutrinos

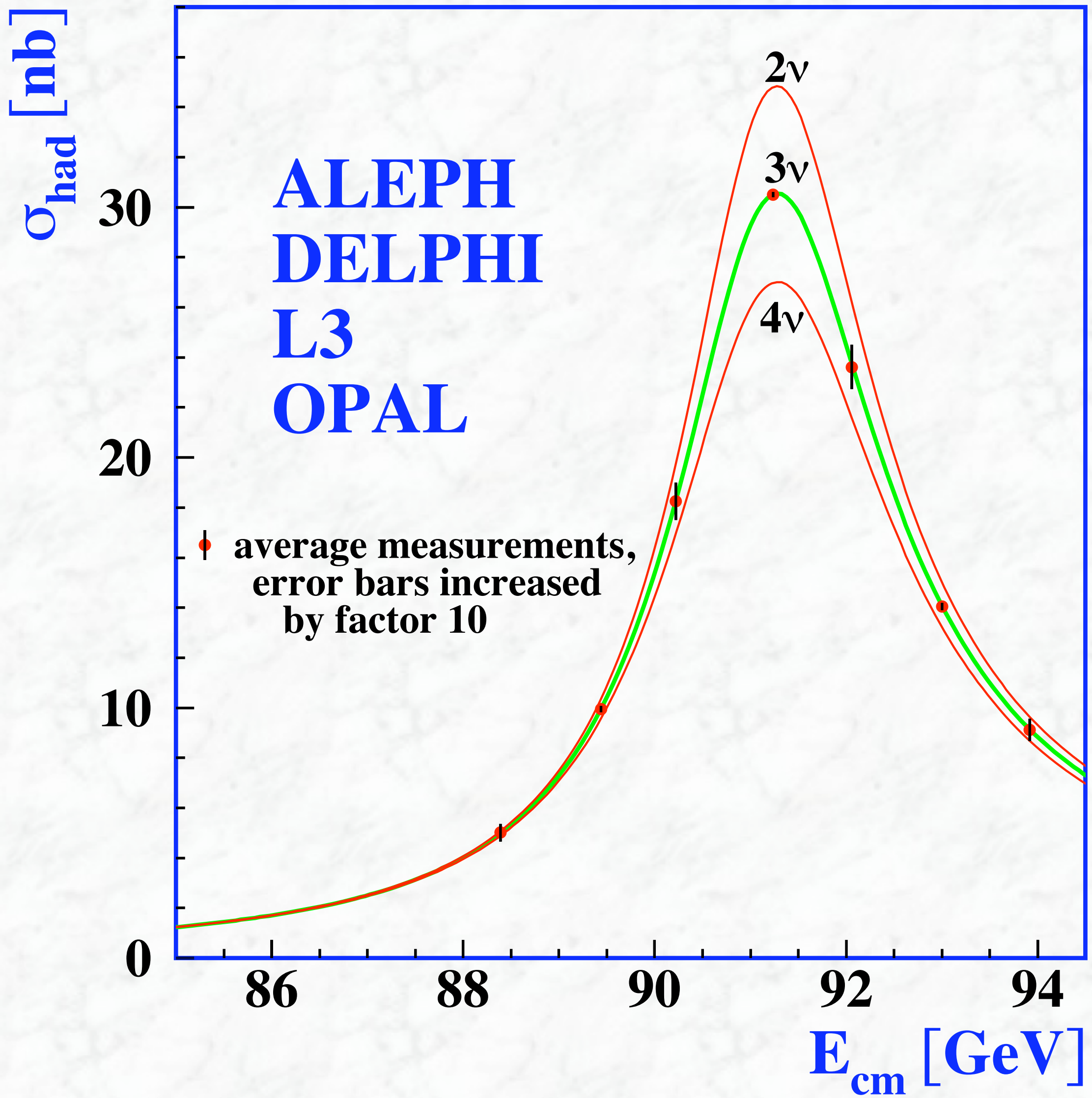

$N_\nu = 2.9840 \pm 0.0082$

Forward-backward asymmetries

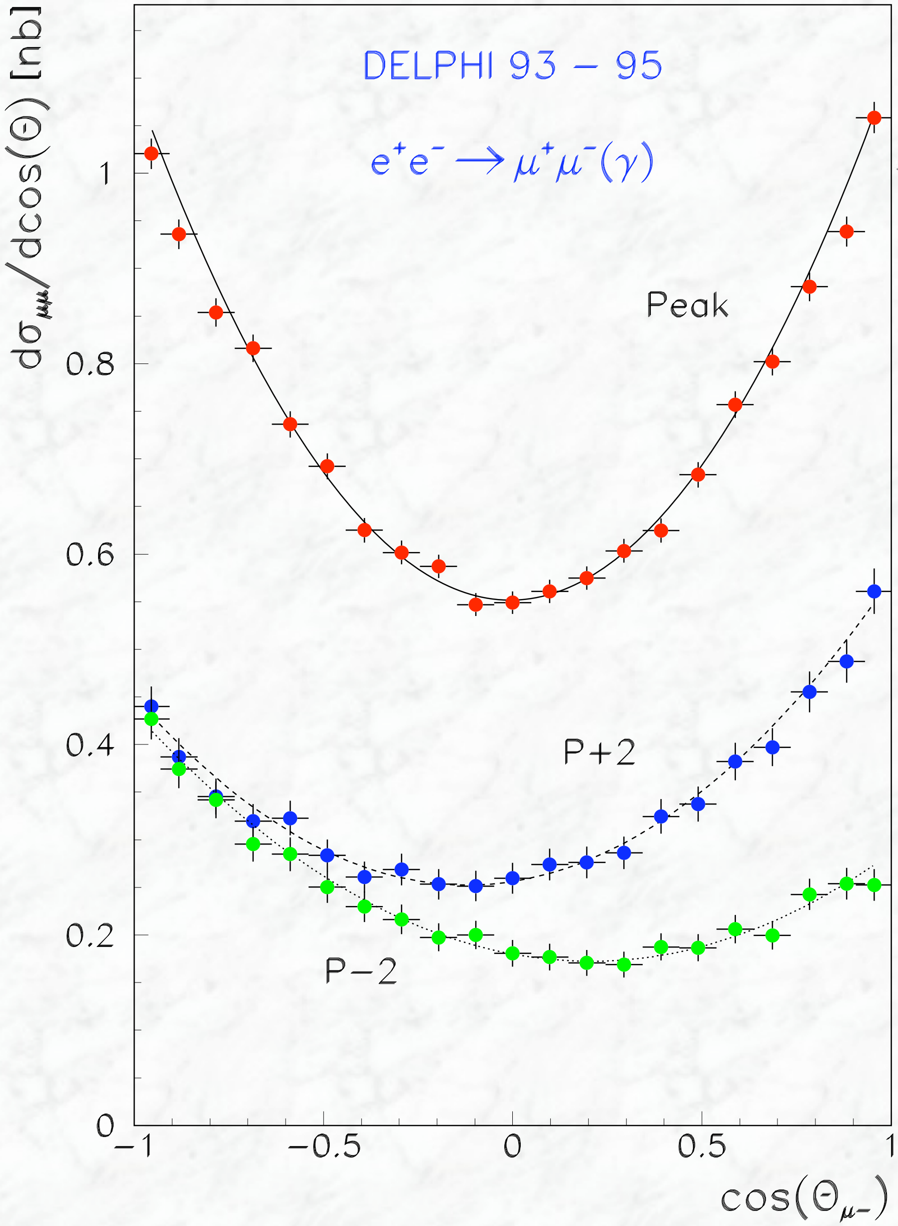

$$F_\gamma(\cos\theta) = Q_e^2 Q_\mu^2 (1+\cos^2\theta) = (1+\cos^2\theta)$$

$$F_{\gamma Z}(\cos\theta) = \frac{Q_e Q_\mu}{4\sin^2\theta_W \cos^2\theta_W}[2g_V^e g_V^\mu (1+\cos^2\theta) + 4g_A^e g_A^\mu \cos\theta]$$

$$F_Z(\cos\theta) = \frac{1}{16\sin^4\theta_W \cos^4\theta_W}[(g_V^{e^2} + g_A^{e^2})(g_V^{\mu^2} + g_A^{\mu^2})(1+\cos^2\theta) +$$

$$8g_V^e g_A^e g_V^\mu g_A^\mu \cos\theta]$$

Terms ∝ cosθ in dσ/dcosθ
→ asymmetry

$$\sigma_{F(B)} = \int_{0(-1)}^{1(0)} \frac{d\sigma}{d\cos\theta} d\cos\theta$$

$$A_{FB} = \frac{\sigma_F - \sigma_B}{\sigma_F + \sigma_B}$$

Forward-backward asymmetries

-comparison between ee and μμ final states-

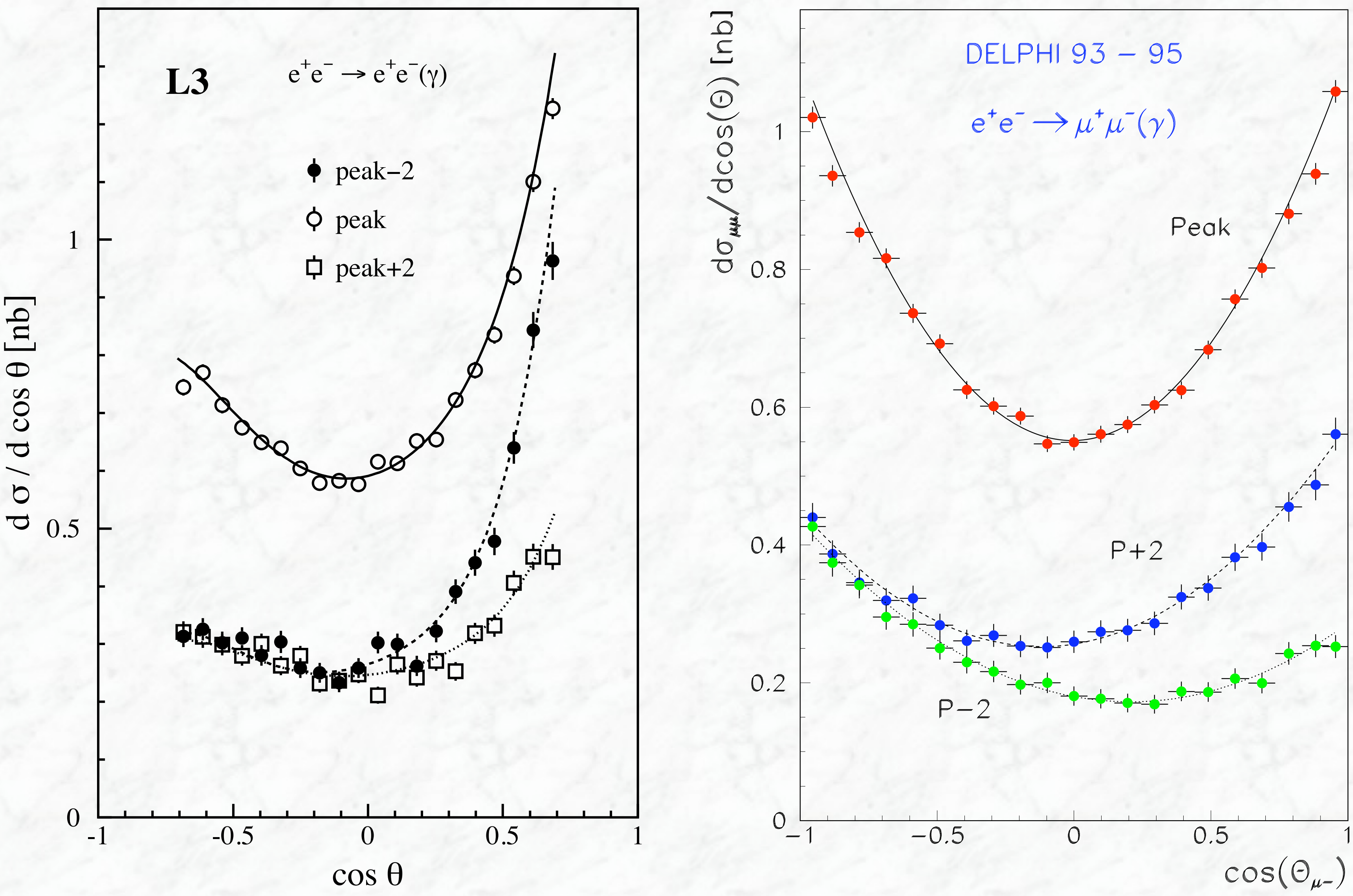

Forward-backward asymmetries and fermion couplings

- Asymmetry at the Z pole (no interference) is small

$$A_{\mathrm{FB}} \sim g_{\mathrm{A}}^{e} g_{\mathrm{V}}^{e} g_{\mathrm{A}}^{f} g_{\mathrm{V}}^{f}$$

since g_V^f is small (in particular for leptons)

- For off-resonance points, the interference term dominates and gives larger contributions

$$A_{\mathrm{FB}} \sim g_{\mathrm{A}}^{e} g_{\mathrm{A}}^{f} \cdot \frac{s(s-M_{\mathrm{Z}}^{2})}{(s-M_{\mathrm{Z}}^{2})^{2}+M_{\mathrm{Z}}^{2}\Gamma_{\mathrm{Z}}^{2}}$$

- A_{FB} can be used for the determination of the fermion couplings

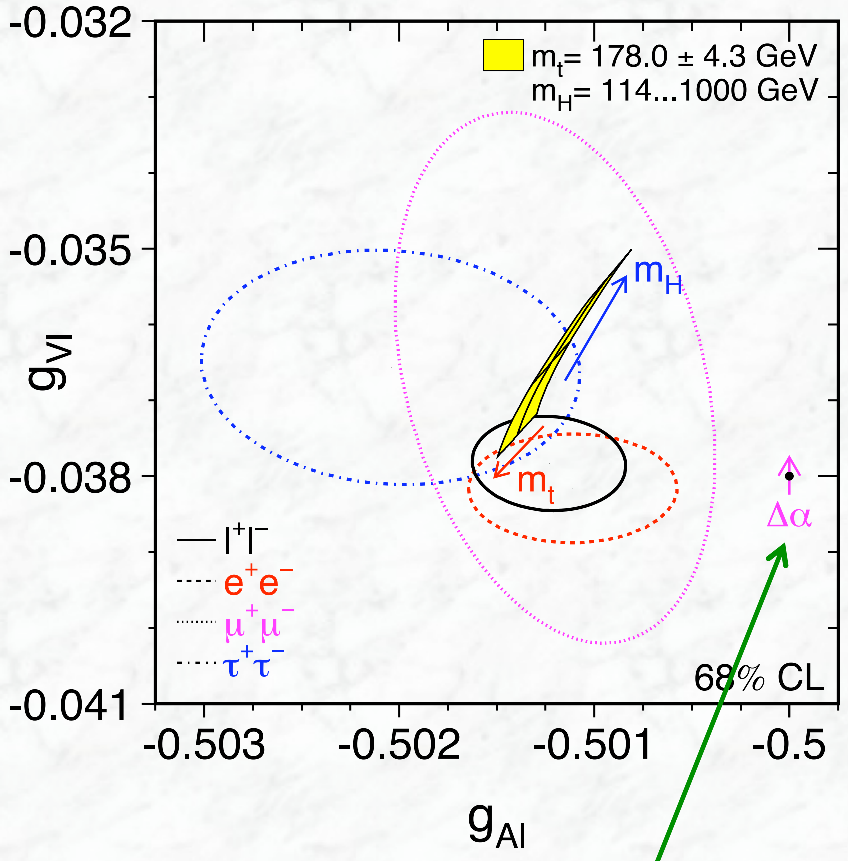

LO Standard Model prediction:
$g_A = T_3$
$g_V = T_3 - 2\,Q \sin^2\theta_W$

Electroweak radiative corrections

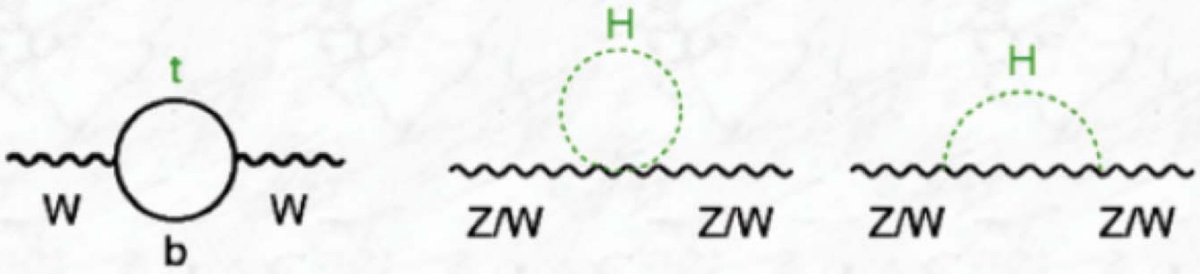

Standard Model relations
(lowest order)

$$\rho = \frac{m_{\mathrm{W}}^2}{m_{\mathrm{Z}}^2 \cos^2 \theta_{\mathrm{W}}} = 1$$

$$\sin^2 \theta_{\mathrm{W}} = 1 - \frac{m_{\mathrm{W}}^2}{m^2 \mathrm{Z}}$$

$$m_{\mathrm{W}}^2 = \frac{\pi \alpha}{\sqrt{2} \sin^2 \theta_{\mathrm{W}} G_{\mathrm{F}}}$$

$$\alpha(0)$$

Relations including
radiative corrections

$$\vec{\rho} = 1 + \Delta\rho$$

$$\sin^2 \theta_{\mathrm{eff}} = (1 + \Delta\kappa) \sin^2 \theta_{\mathrm{W}}$$

$$m_{\mathrm{W}}^2 = \frac{\pi \alpha}{\sqrt{2} \sin^2 \theta_{\mathrm{W}} G_{\mathrm{F}}} \cdot \frac{1}{(1 - \Delta r)}$$

$$\alpha(m_{\mathrm{Z}}^2) = \frac{\alpha(0)}{1 - \Delta\alpha}$$

$$\Delta\alpha = \Delta\alpha_{\mathrm{lepl}} + \Delta\alpha_{\mathrm{top}} + \Delta\alpha_{\mathrm{had}}^{(5)}$$

$$\Delta\rho, \Delta\kappa, \Delta r = f(m_t^2, \log(m_{\mathrm{H}}), \ldots)$$

Results of electroweak precision tests at LEP (cont.)

partial decay width versus $\sin^2 \theta_W$:

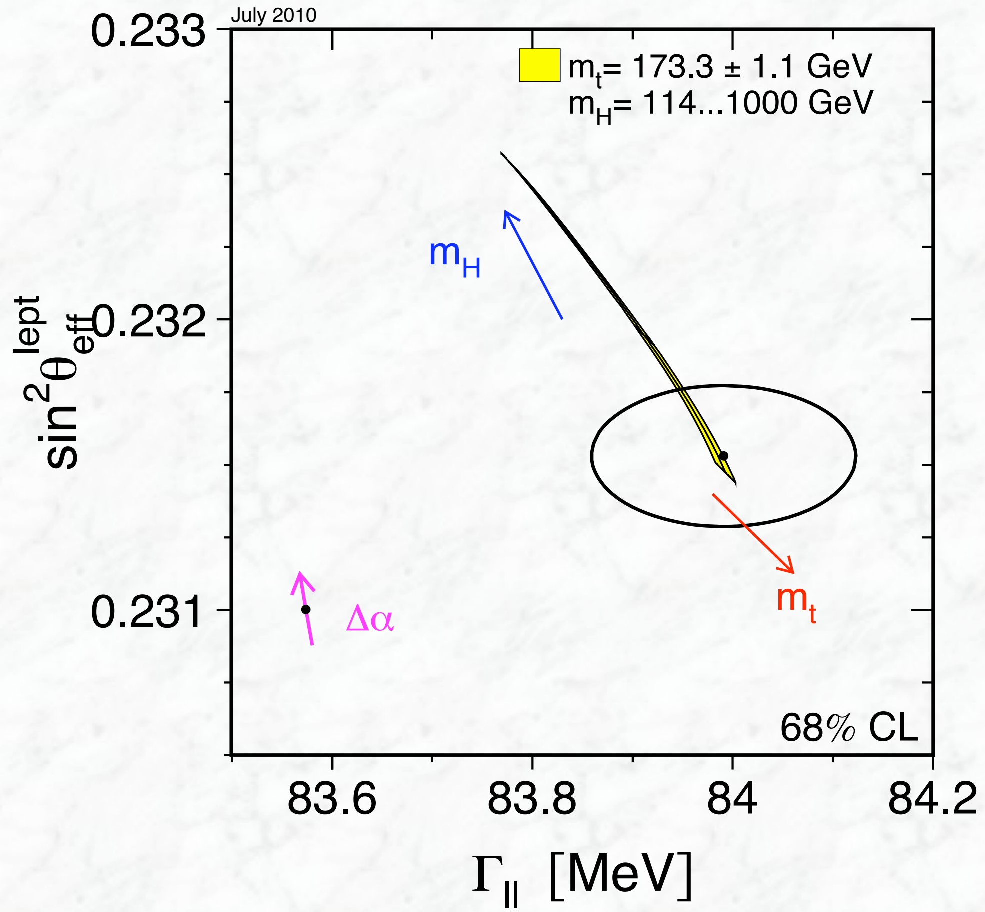

Results of electroweak precision tests at LEP (cont.)

Summary of results:

- All measurements in agreement with the Standard Model
- They can be described with a limited set of parameters

	Measurement	Fit
$\Delta\alpha_{had}^{(5)}(m_Z)$	0.02758 ± 0.00035	0.02768
m_Z [GeV]	91.1875 ± 0.0021	91.1874
Γ_Z [GeV]	2.4952 ± 0.0023	2.4959
σ_{had}^{0} [nb]	41.540 ± 0.037	41.479
R_l	20.767 ± 0.025	20.742
$A_{fb}^{0,l}$	0.01714 ± 0.00095	0.01645
$A_l(P_\tau)$	0.1465 ± 0.0032	0.1481
R_b	0.21629 ± 0.00066	0.21579
R_c	0.1721 ± 0.0030	0.1723
$A_{fb}^{0,b}$	0.0992 ± 0.0016	0.1038
$A_{fb}^{0,c}$	0.0707 ± 0.0035	0.0742
A_b	0.923 ± 0.020	0.935
A_c	0.670 ± 0.027	0.668
A_l(SLD)	0.1513 ± 0.0021	0.1481
$\sin^2\theta_{eff}^{lept}(Q_{fb})$	0.2324 ± 0.0012	0.2314
m_W [GeV]	80.399 ± 0.023	80.379
Γ_W [GeV]	2.085 ± 0.042	2.092
m_t [GeV]	173.3 ± 1.1	173.4

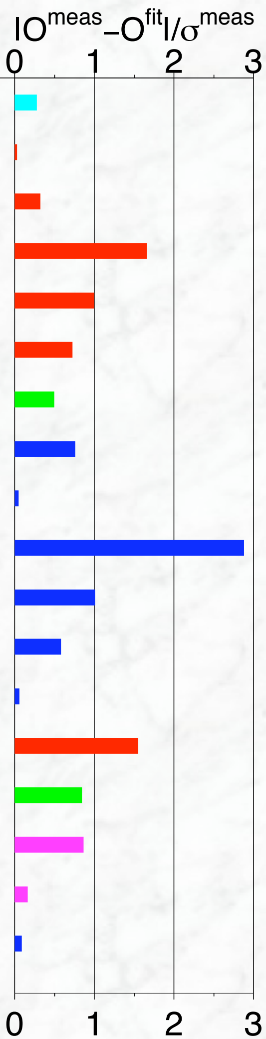

July 2010

6.3 W/Z production at hadron colliders

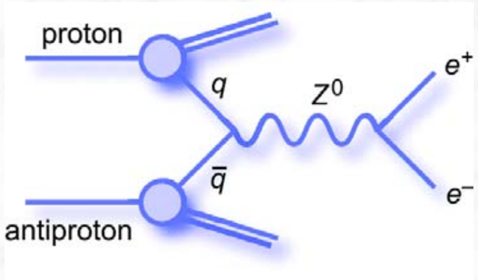

QCD at work

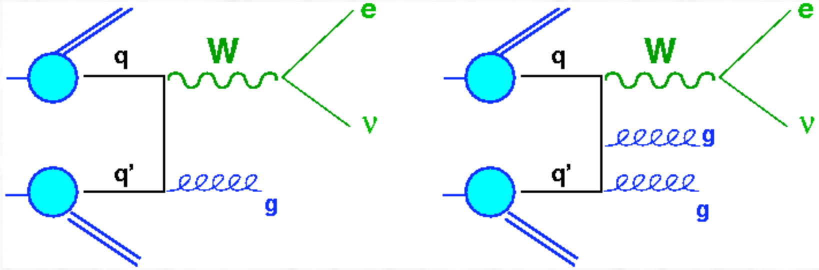

- Important test of NNLO Drell-Yan QCD prediction for the total cross section
- Test of perturbative QCD in high p_T region
  (jet multiplicities, p_T spectra,….)
- Tuning and „calibration" of Monte Carlos for background predictions in searches
  at the LHC

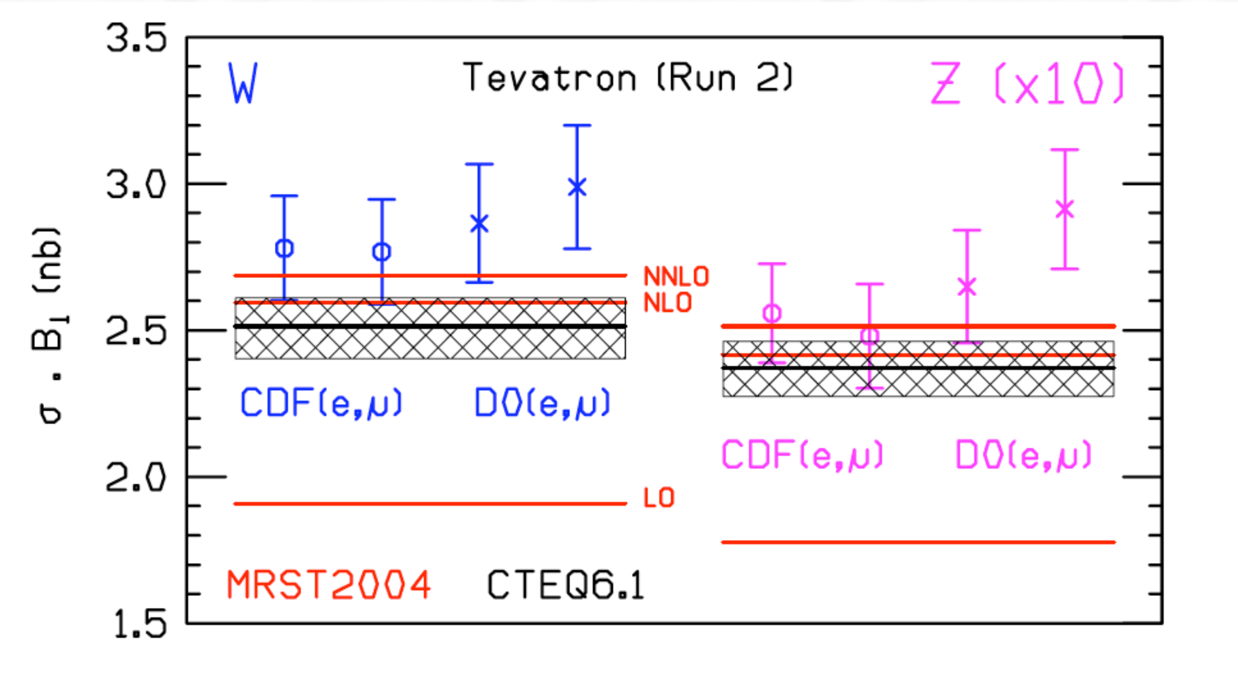

Predictions for the W and Z boson total cross sections at the Tevatron, using the MRST2004 and CTEQ pdfs, compared with measurements from the CDF and D0 collaborations. The predictions are shown at LO, NLO, and NNLO. For the NLO prediction the accompanying pdf uncertainties are shown as band.

W boson production cross sections at the LHC ($\sqrt{s}$ = 7 TeV)

Program	Non-standard parameters	W charge	Cross Section (pb)
Cross sections for the full kinematic regime			
FEWZ	MSTW2008NNLO	W^+	6160^{+49}_{-55} (scale) ± 111 (PDF) ± 74 (α_s)
		W^-	4301^{+34}_{-34} (scale) ± 69 (PDF) ± 52 (α_s)
		$W^+ + W^-$	10461^{+84}_{-94} (scale) ± 167 (PDF) ± 126 (α_s)
ZWPRODMS	MSTW2008NNLO	W^+	6189^{+33}_{-50} (scale) ± 105 (PDF) ± 67 (α_s)
		W^-	4316^{+25}_{-33} (scale) ± 72 (PDF) ± 44 (α_s)
		$W^+ + W^-$	10506^{+58}_{-83} (scale) ± 173 (PDF) ± 111 (α_s)
Cross sections for the kinematic regime of Eq. 1			
FEWZ	MSTW2008NNLO	W^+	2907
		W^-	1927
		$W^+ + W^-$	4833

Predictions for the W → lν cross section at NNLO, calculated for the full kinematic range as well as in the fiducial region (see below).

Major uncertainties: renormalization and factorization scale (~ ±1%)
parton distribution functions (~ ±2)%
uncertainties of α_s (~ ±1%)

Fiducial region: PT(l) > 20 GeV, η < 2.47, excluding 1.37 < η < 1.52
E_T^{miss} > 25 GeV
m_T > 40 GeV

Z boson production cross sections at the LHC ($\sqrt{s}$ = 7 TeV)

Program	Non-standard parameters	Mass range (GeV)	Cross Section (pb)
Cross section for the full kinematic regime			
FEWZ	MSTW2008NNLO	> 60	989^{+5}_{-7} (scale) ± 16 (PDF) ± 10 (α_s)
		$60 - 120$	978^{+5}_{-7} (scale) ± 16 (PDF) ± 10 (α_s)
		$66 - 116$	964^{+5}_{-7} (scale) ± 15 (PDF) ± 10 (α_s)
		$70 - 110$	952^{+5}_{-7} (scale) ± 15 (PDF) ± 10 (α_s)
		$80 - 100$	904^{+5}_{-6} (scale) ± 14 (PDF) ± 9 (α_s)
		only Z, full range	970^{+5}_{-7} (scale) ± 15 (PDF) ± 10 (α_s)
ZWPRODMS		only Z, full range	974^{+5}_{-6} (scale) ± 16 (PDF) ± 10 (α_s)
Cross section for the kinematic regime specified in Eq. 2			
FEWZ	MSTW2008NNLO	$66 - 116$	420

Predictions for the Z / γ^* → ll cross section at NNLO, calculated for the full kinematic range as well as in the fiducial region (see below).

Major uncertainties: renormalization and factorization scale (~ ±1%)
parton distribution functions (~ ±1.5)%
uncertainties of α_s (~ ±1%)

Fiducial region: PT(l) > 20 GeV, η < 2.47, excluding 1.37 < η < 1.52
66 < m_{ll} < 116 GeV

6.4 Test of QCD in W/Z production at hadron colliders

As explained, leptons, photons and missing transverse energy are key signatures at hadron colliders

→ Search for leptonic decays: $W \rightarrow \ell \nu$ (large $P_T(\ell)$, large P_T^{miss})
$Z \rightarrow \ell \ell$

More difficult: $W \rightarrow \tau \nu \rightarrow$ had $\nu\nu$ $Z \rightarrow \tau \tau \rightarrow e(\mu)\, \nu\nu$ had ν

Ingredients for a cross-section measurement:

$$\sigma = \frac{N_{sel} - N_{back}}{L \cdot \varepsilon \cdot \eta}$$

where: N_{sel} = number of selected events
N_{back} = number of background events in selected events

L = integrated luminosity (measured from machine, reference process)
ε = detection efficiency
η = acceptance of fiducial cuts ($P_T(l)$, E_T^{miss}, M_T, m_{ll},….)

How do W and Z events look like ?

A bit of history: one of the first W and Z events seen (UA2 experiment)

W/Z discovery by the UA1 and UA2 experiments at CERN (1983/84)

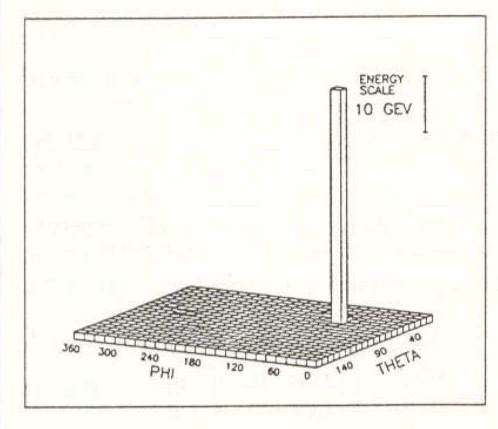

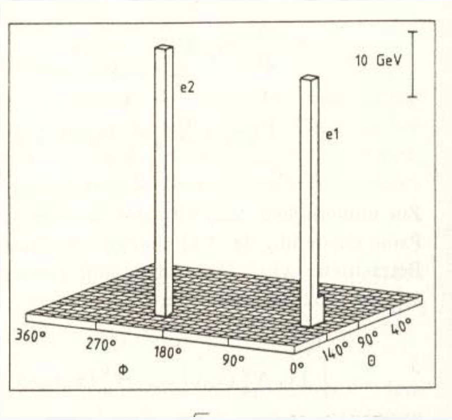

Carlo Rubbia (left, UA1) and
Luigi Di Lella (right, UA2)

Transverse momentum of
the electrons

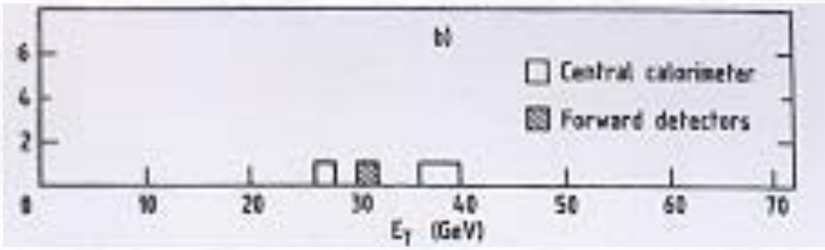

Today's W / Z → eν / ee signals

CDF Experiment, Fermilab

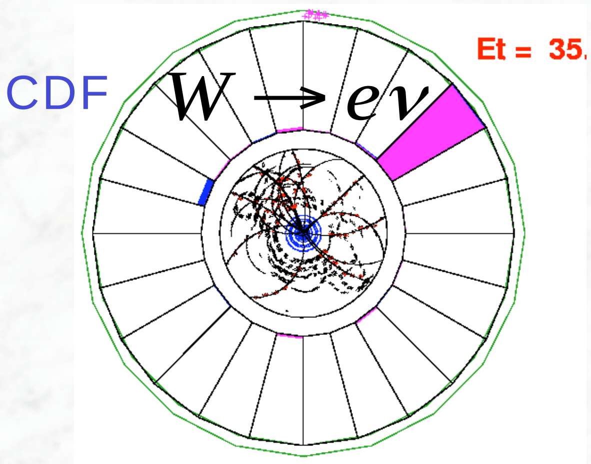

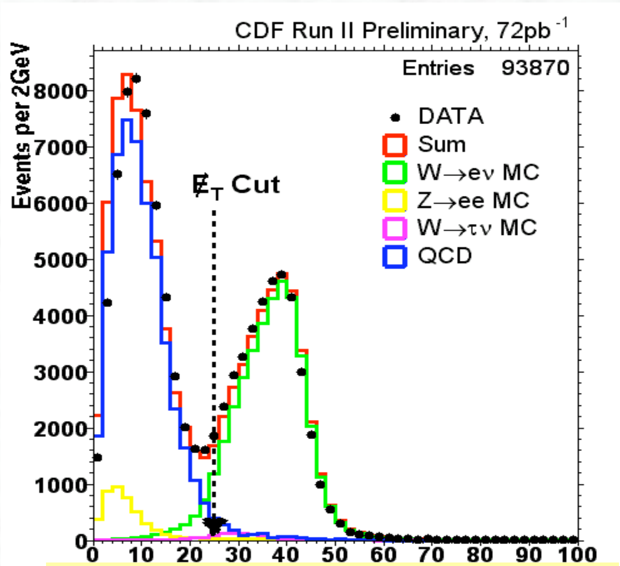

missing transverse momentum P_T^{miss} (GeV/c)

Trigger:

- Electron candidate > 20 GeV/c

Electrons:

- Isolated el.magn. cluster in the calorimeter
- P_T> 25 GeV/c
- Shower shape consistent with expectation for electrons
- Matched with tracks

Z → ee

- 70 GeV/c^2 < m_{ee} < 110 GeV/c^2

W → eν

- Missing transverse momentum > 25 GeV/c

Z→ ℓℓ cross sections

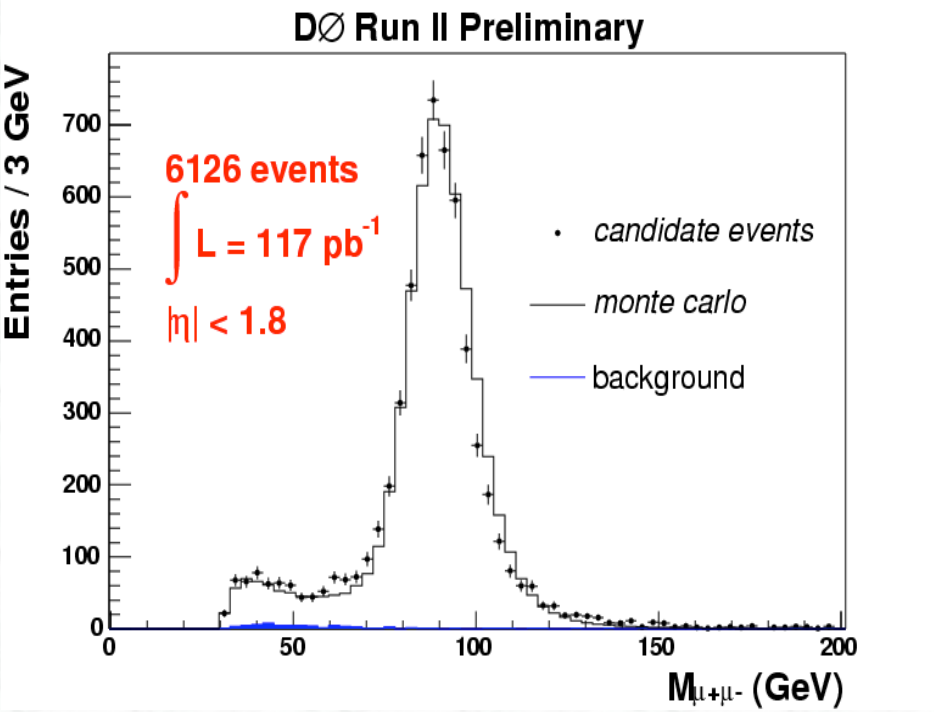

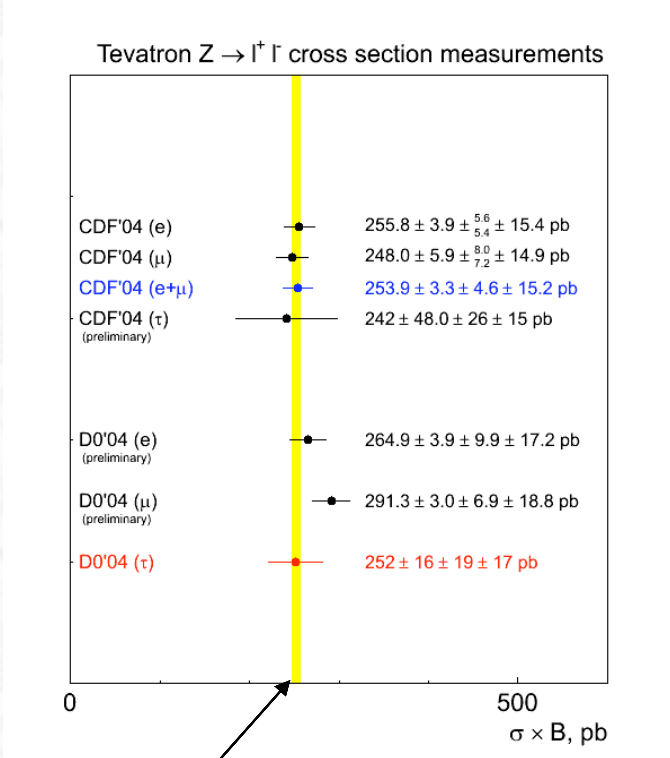

Good agreement with NNLO QCD calculations, QCD corrections are large: factor ~ 1.25

C.R.Hamberg et al, Nucl. Phys. B359 (1991) 343.

Precision is limited by systematic effects (uncertainties on luminosity, parton densities,...)

W → ℓν Cross Section

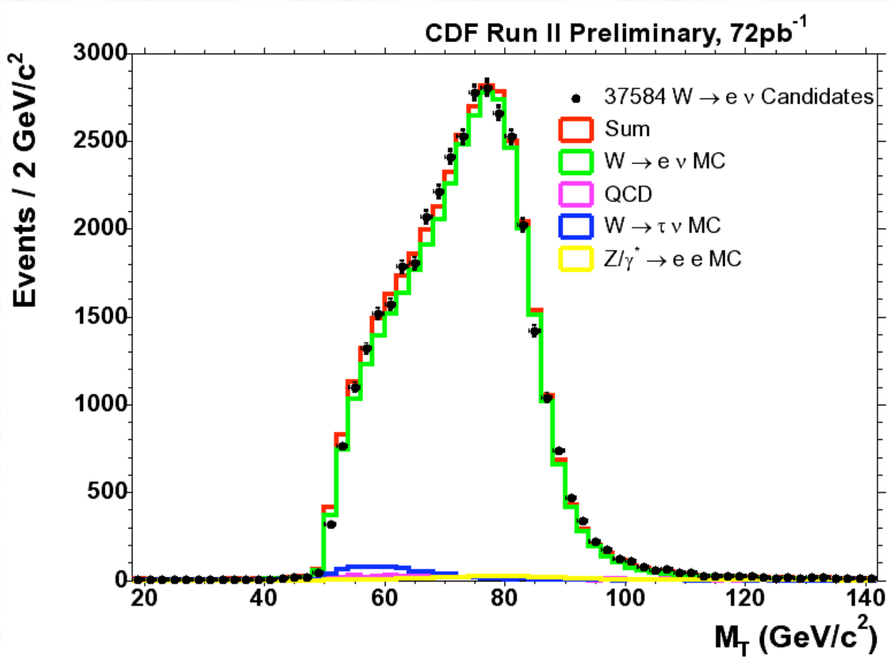

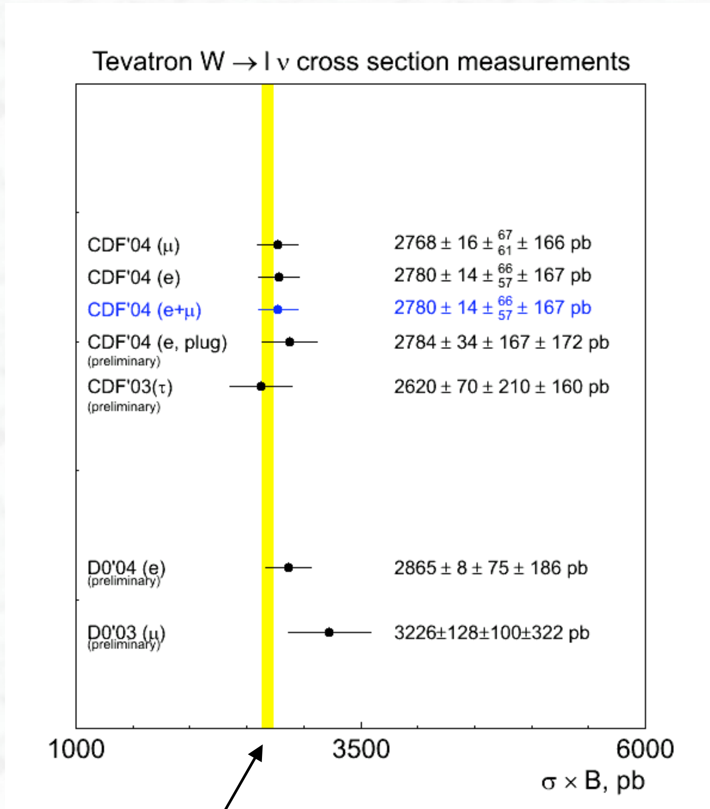

$$M_W^T = \sqrt{2 \cdot P_T^l \cdot P_T^\nu \cdot \left(1 - \cos\Delta\phi^{l,\nu}\right)}$$

Note: the longitudinal component of the neutrino cannot be measured
→ only transverse mass can be reconstructed

Good agreement with NNLO QCD calculations
C.R.Hamberg et al, Nucl. Phys. B359 (1991) 343.

Precision is limited by systematic effects (uncertainties on luminosity, parton densities,...)

Comparison between measured W/Z cross sections and theoretical prediction (QCD)

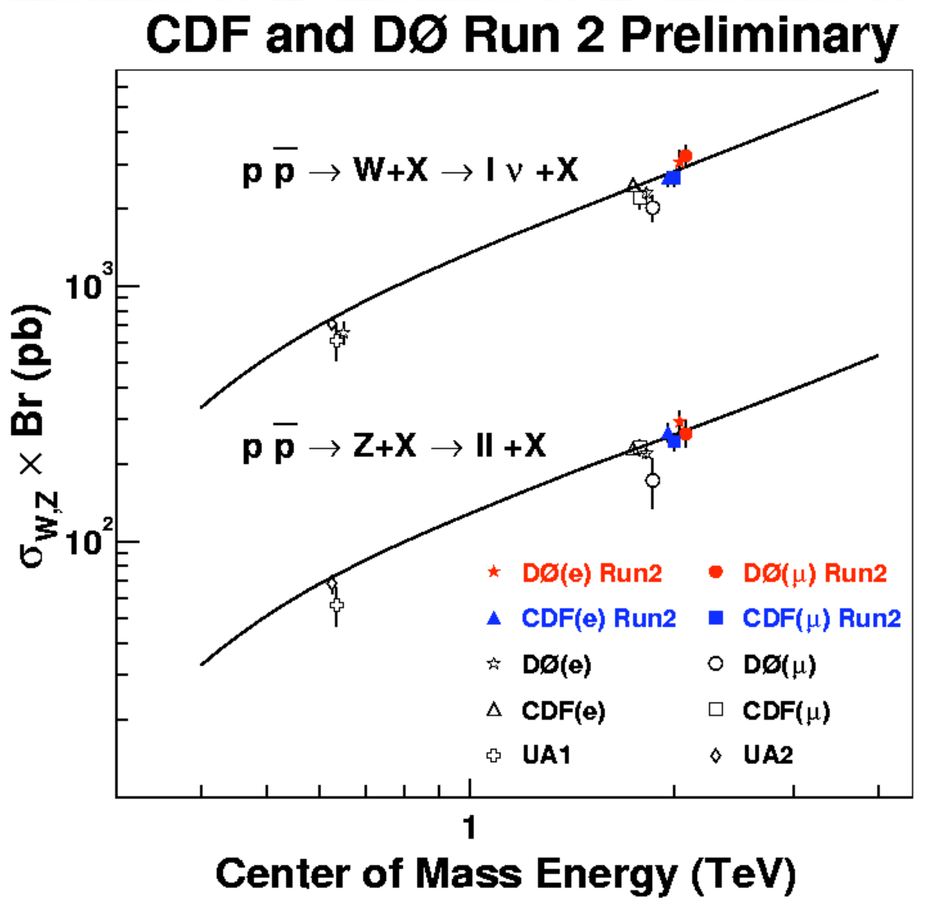

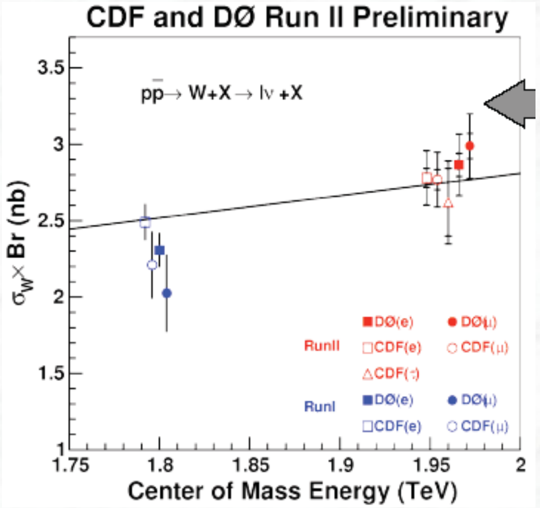

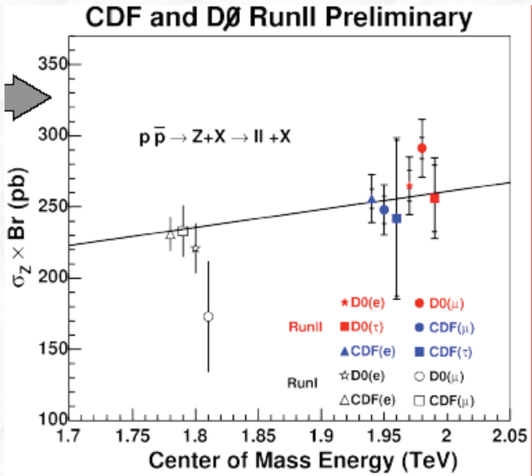

C. R. Hamberg, W.L. van Neerven and T. Matsuura, Nucl. Phys. B359 (1991) 343

First measurements of W/Z production at the LHC -early ATLAS data: 0.31 pb^{-1} (Summer 2010)

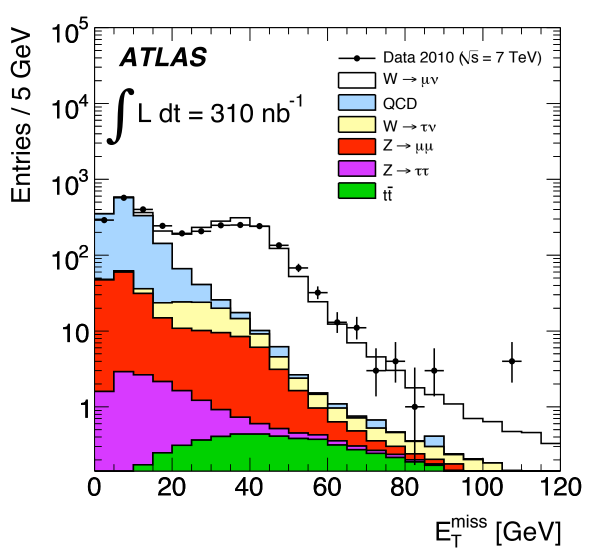

Distributions of the missing transverse energy, E_T^{miss}, of muon candidates for data and Monte-Carlo simulation, broken down into the signal and various background components.

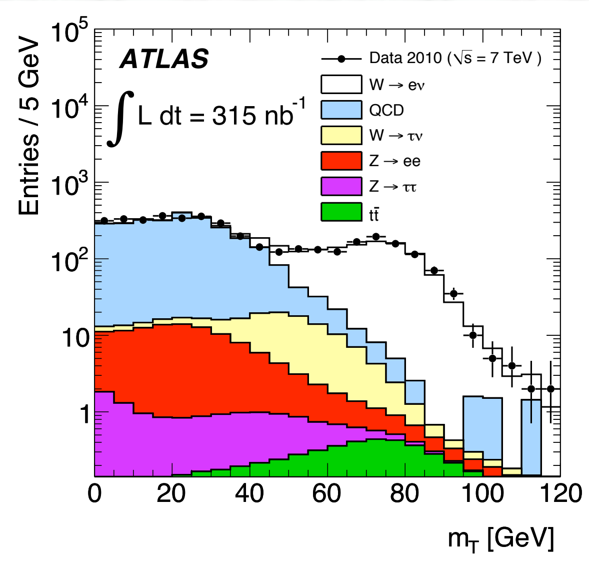

Distributions of the transverse mass, m_T, of the electron-E_t^{miss} system without an E_t^{miss} requirement. The data are compared to Monte-Carlo simulation, broken down into the signal and various background components.

First measurements of W/Z production at the LHC
-CMS data from 2010: 36 pb^{-1} -

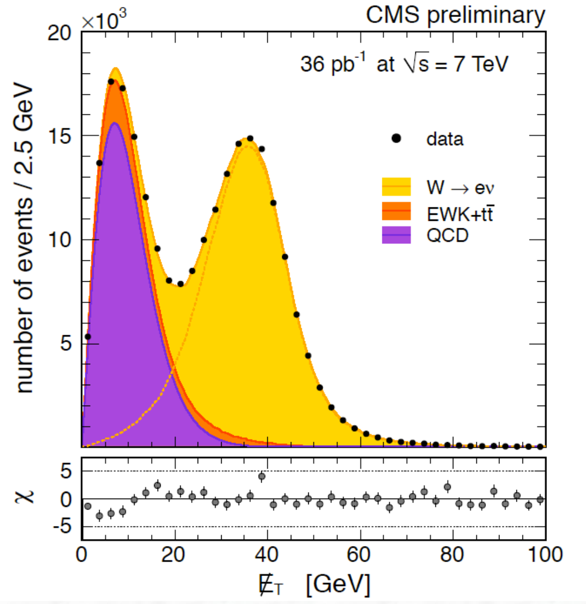

Distributions of the missing transverse energy, E_T^{miss}, of electron candidates for data and Monte-Carlo simulation, broken down into the signal and various background components.

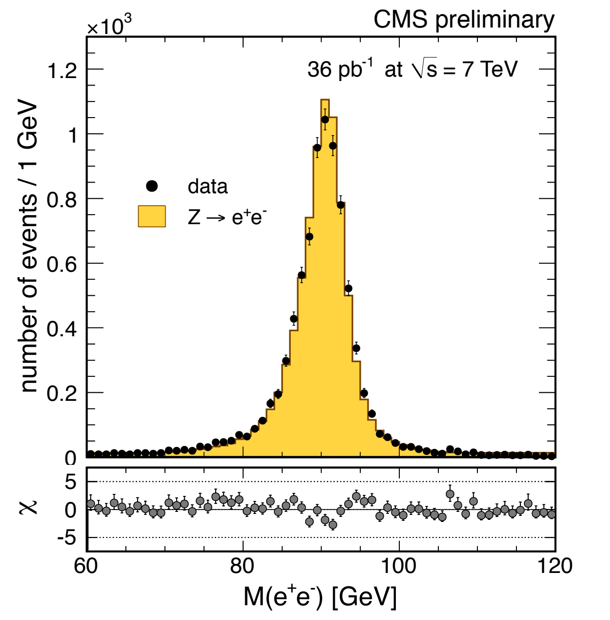

Distributions of the invariant di-electron mass, m_{ee}, for events passing the Z selection. The data are compared to Monte-Carlo simulation, the background is very small.

W and Z production cross sections at LHC

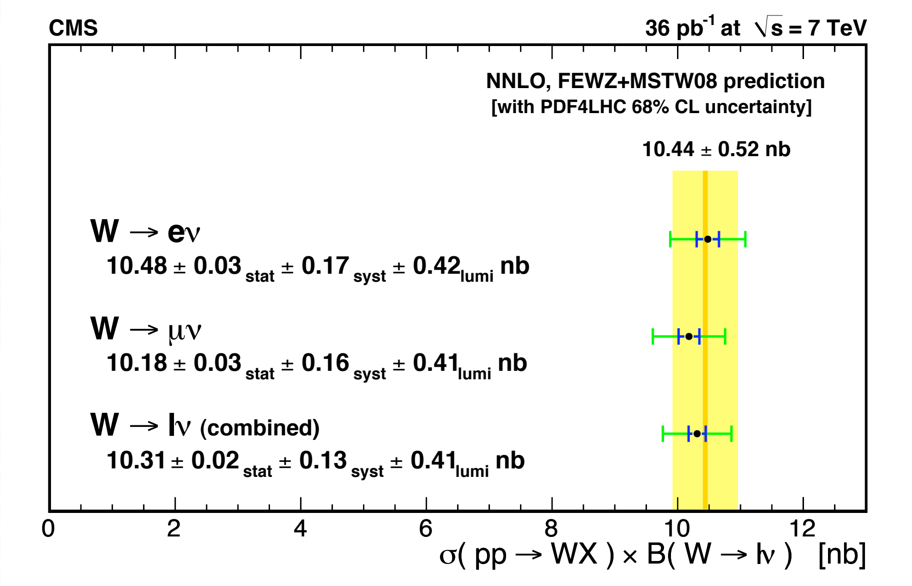

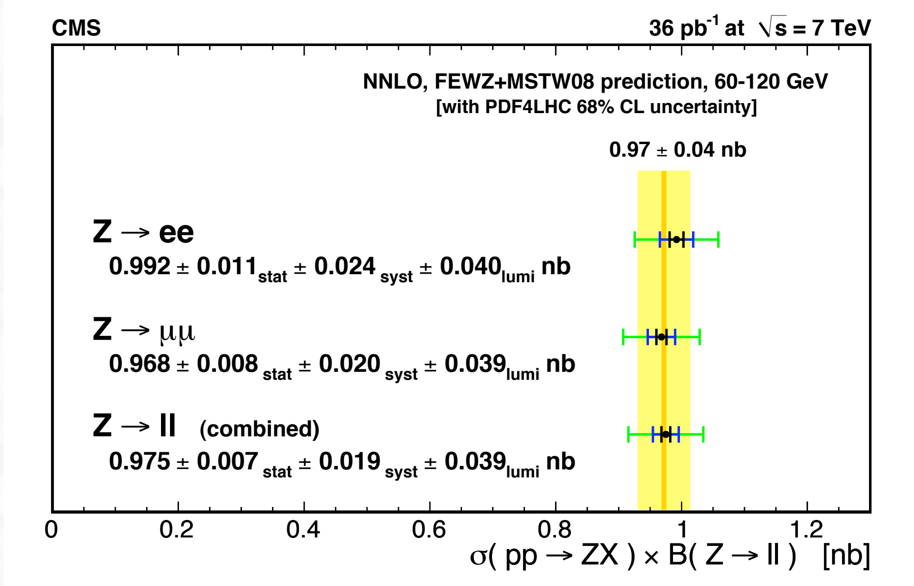

The measured values of σ_W x BR(W → lν) and σ_Z x BR(Z → ll) for W and Z production in the CMS experiment, compared to the theoretical predictions based on NNLO QCD calculations. Results are shown for the electron and muon final states as well as for their combination. The error bars represent successively the statistical, the statistical plus systematic and the total uncertainties (statistical, systematic and luminosity).
All uncertainties are added in quadrature.

W production cross sections at hadron colliders

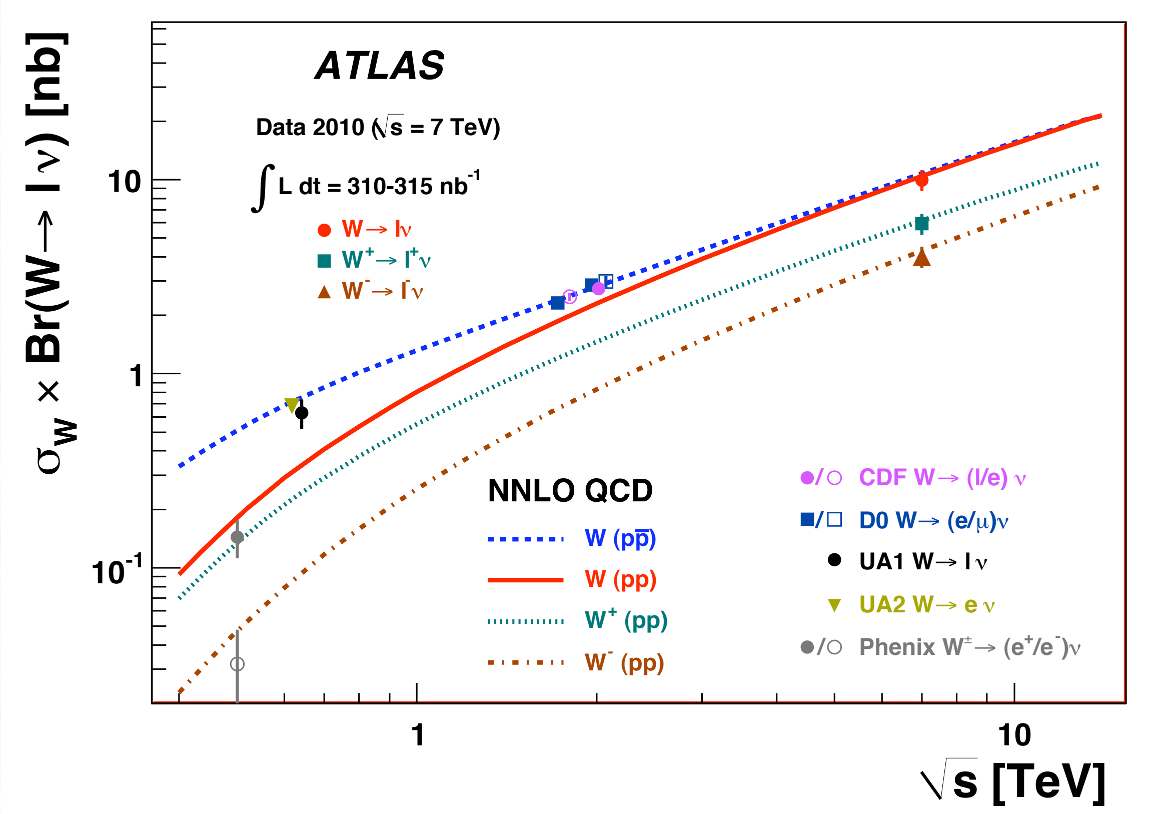

The measured values of σ_W x BR(W → l ν) for W+, W- and for their sum compared to the theoretical predictions based on NNLO QCD calculations. Results are shown for the combined electron-muon results. The predictions are shown for both proton-proton (W+,W- and their sum) and proton-antiproton colliders (W) as a function of root(s). In addition, previous measurements at proton-antiproton and proton-proton colliders are shown. The data points at the various energies are staggered to improve readability. The CDF and D0 measurements are shown for both Tevatron collider energies, √s = 1.8 TeV and √s = 1.96 TeV. All data points are displayed with their total uncertainty. The theoretical uncertainties are not shown.

Z production cross sections at hadron colliders

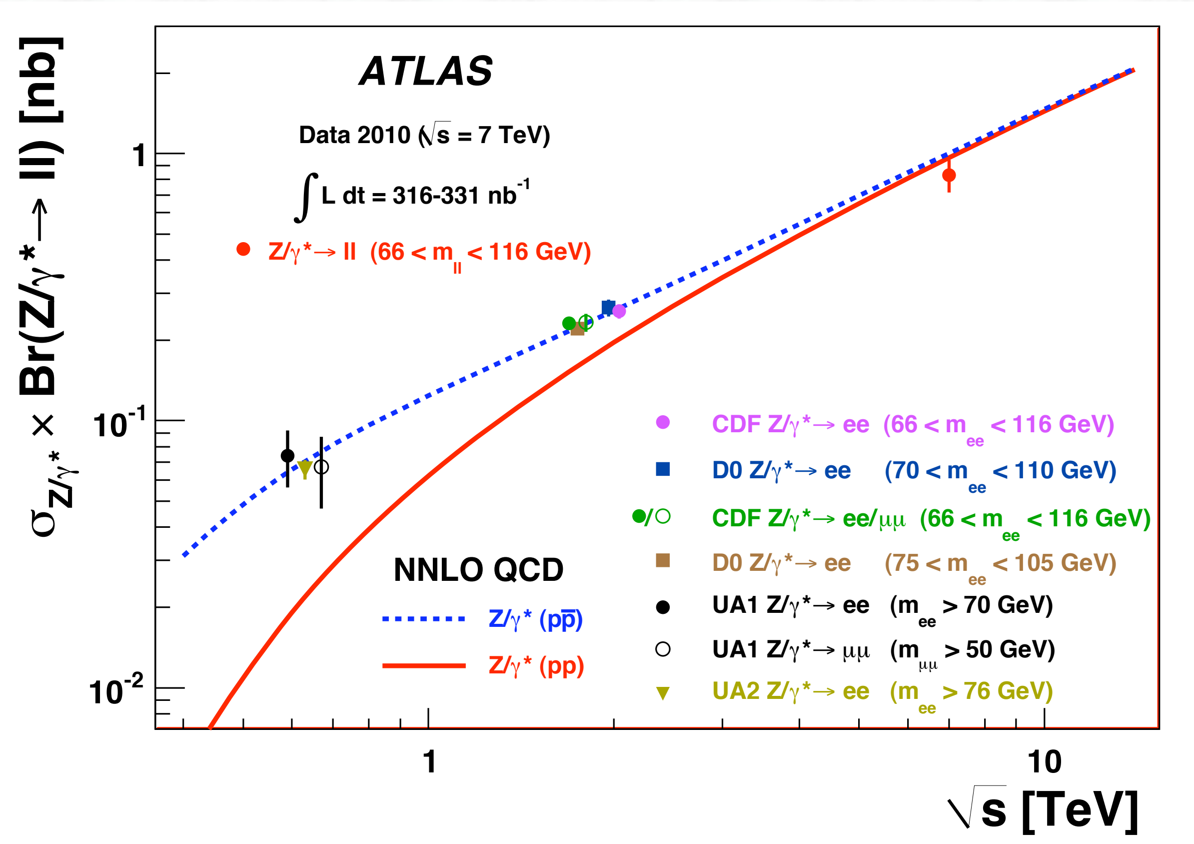

The measured values of σ_Z x BR(Z→ ll) where the electron and muon channels have been combined, compared to the theoretical predictions based on NNLO QCD calculations. The predictions are shown for both proton-proton and proton-antiproton colliders as a function of √s. In addition, previous measurements at proton-antiproton colliders are shown. The data points at the various energies are staggered to improve readability. The CDF and D0 measurements are shown for both Tevatron collider energies, √s= 1.8 TeV and √s = 1.96 TeV. All data points are displayed with their total uncertainty. The theoretical uncertainties are not shown.

W cross sections in ATLAS, charge separated

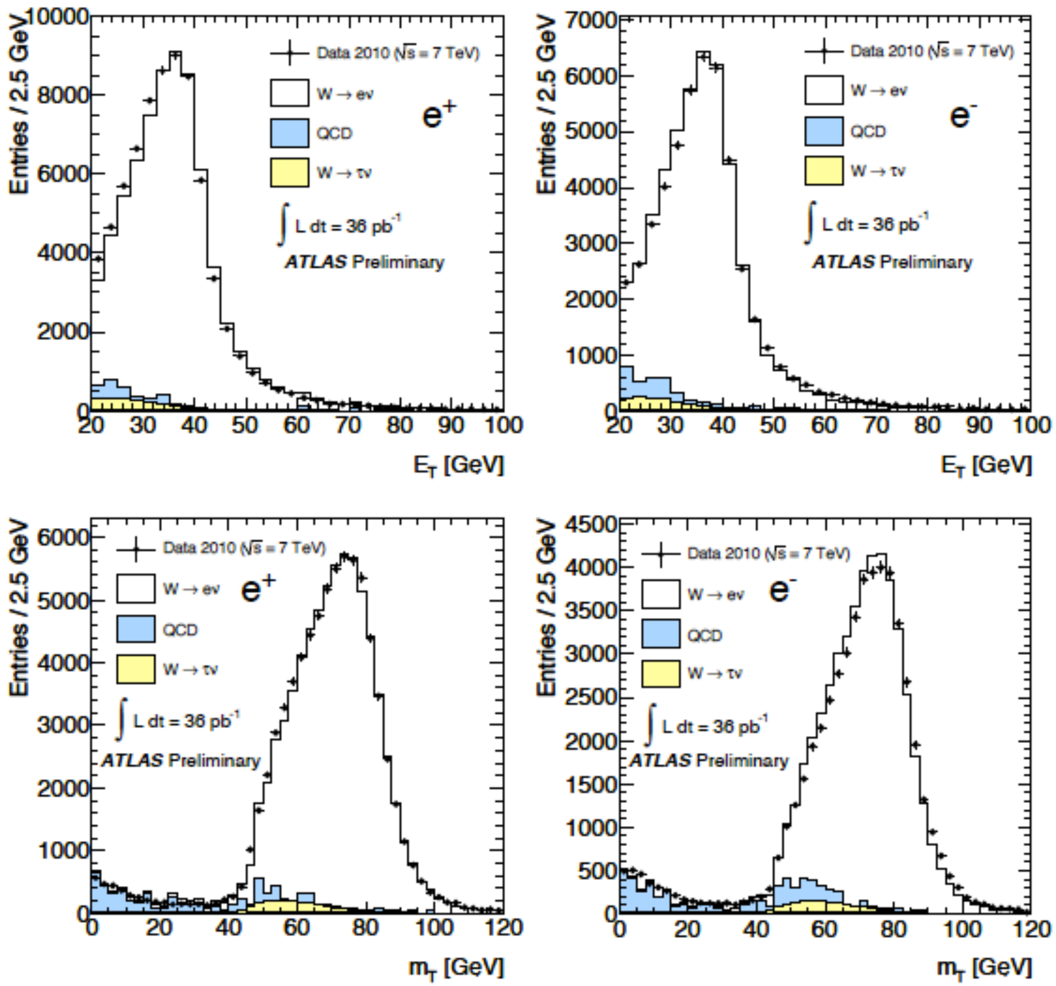

Full ATLAS data set from 2010

L = 36 pb^{-1}

Distribution of transverse energy (top) and transverse mass m_T (bottom) of the electron in the selected W to electron candidate events after all cuts for positive (left) and negative (right) charge. The simulated distributions are normalised to the data.

W^+ and W^- production cross sections at LHC

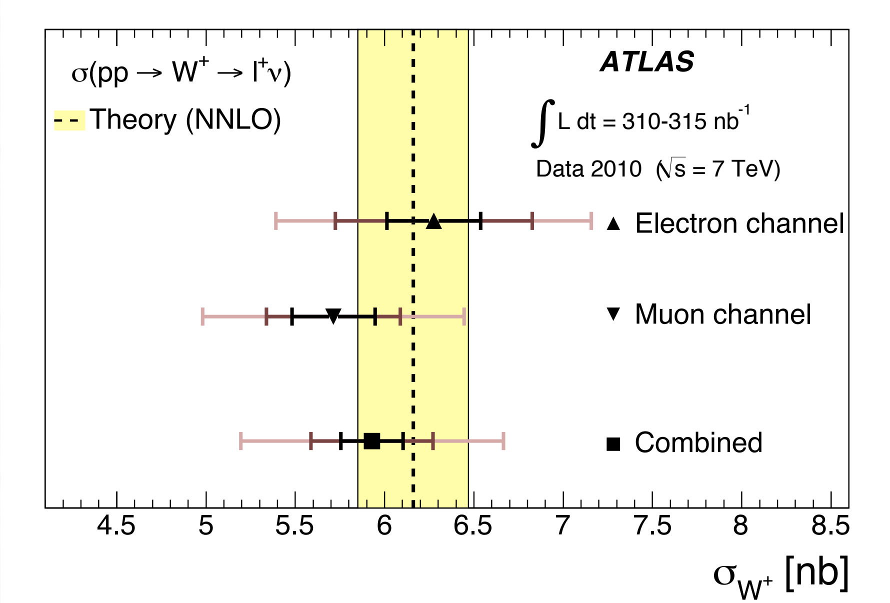

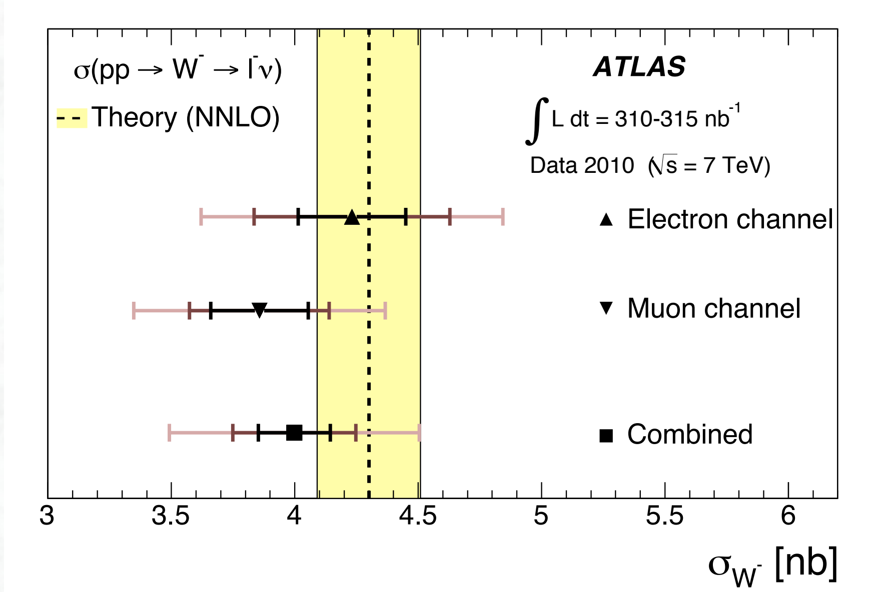

The measured values of sigma_W x BR(W to lnu) for W+ and W- compared to the theoretical predictions based on NNLO QCD calculations. Results are shown for the electron and muon final states as well as for their combination. The error bars represent successively the statistical, the statistical plus systematic and the total uncertainties (statistical, systematic and luminosity). All uncertainties are added in quadrature.

W cross sections at the LHC, charge separated

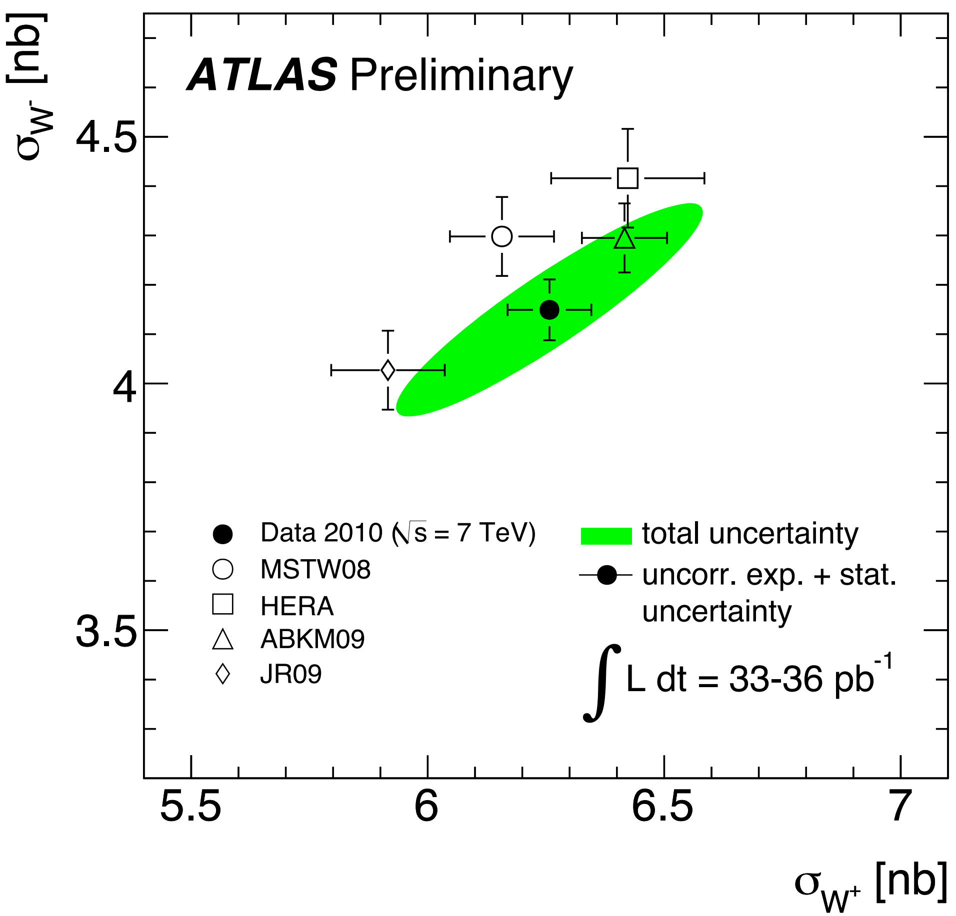

Full ATLAS data set from 2010

L = 36 pb^{-1}

Measured and predicted W- vs. W+ cross sections times leptonic branching ratios. The systematic uncertainties on the lumninosity, on the acceptance extrapolation and on the missing transverse energy scale and resolution are treated as fully correlated. The projections of the ellipse to the axes correspond to one standard deviation uncertainty of the cross sections. The uncertainties of the predictions are the PDF uncertainties only. There is an additional uncertainty of the theoretical cross sections due to the uncertainty of the strong coupling constant, at the level of 2% for a 1% error on the coupling constant itself, which is not included in the theory error bars.

W cross sections at the LHC, charge separated

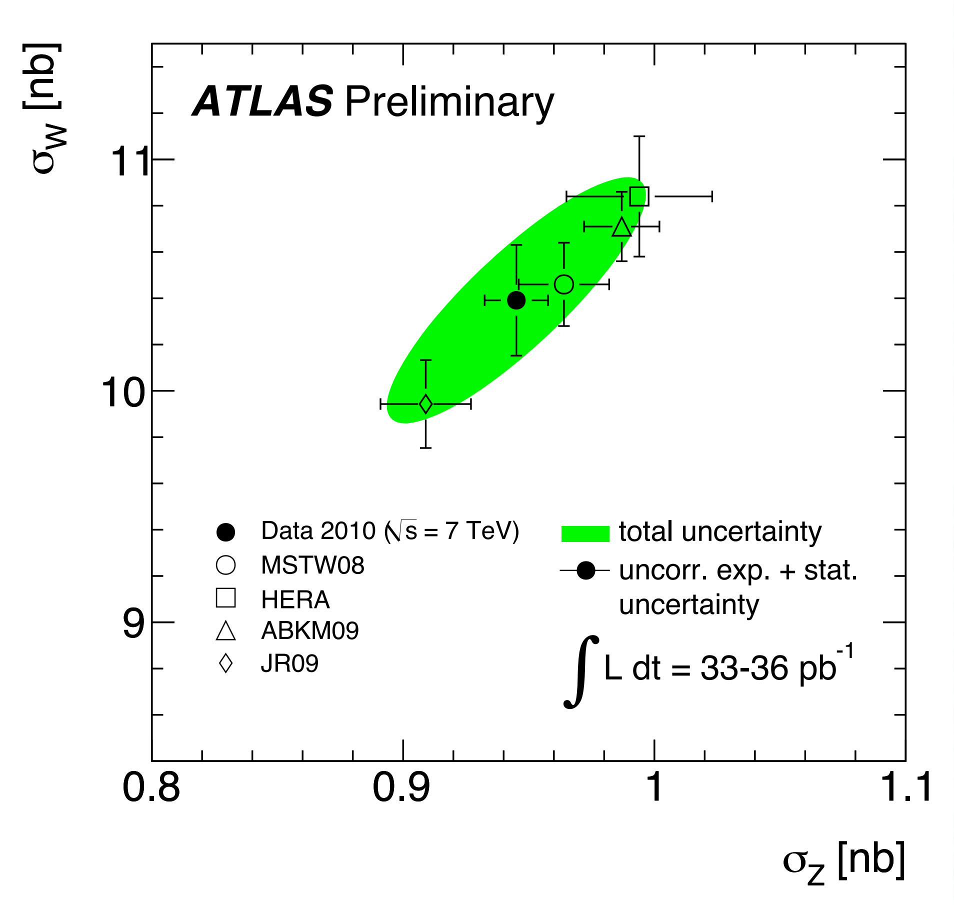

Full ATLAS data set from 2010

L = 36 pb^{-1}

Measured and predicted W vs. Z cross sections times leptonic branching ratios. The systematic uncertainties on the lumninosity, on the acceptance extrapolation and on the missing transverse energy scale and resolution are treated as fully correlated. The projections of the ellipse to the axes correspond to one standard deviation uncertainty of the cross sections. The uncertainties of the predictions are the PDF uncertainties only. There is an additional uncertainty of the theoretical cross sections due to the uncertainty of the strong coupling constant, at the level of 2% for a 1% error on the coupling constant itself, which is not included in the theory error bars.

W charge asymmetry as a function of pseudorapidity

$$A_\mu = \frac{d\sigma_{W\mu^+}/d\eta_\mu - d\sigma_{W\mu^-}/d\eta_\mu}{d\sigma_{W\mu^+}/d\eta_\mu + d\sigma_{W\mu^-}/d\eta_\mu}$$

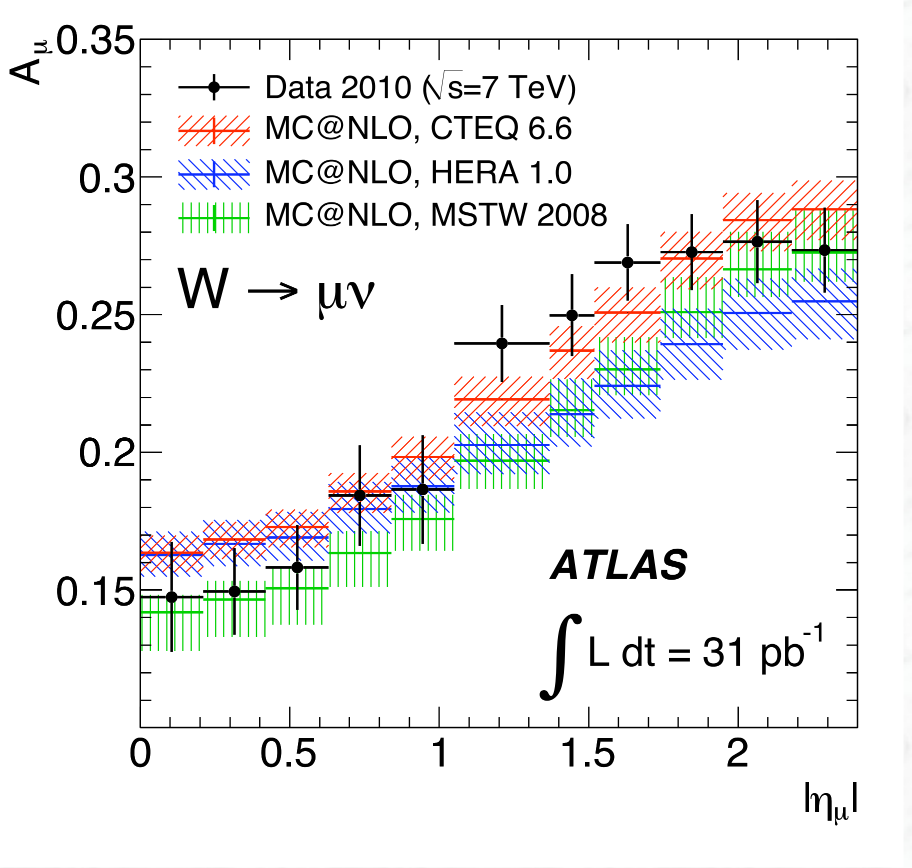

The muon charge asymmetry from W-boson decays in bins of absolute pseudorapidity. The kinematic requirements applied are muon pT > 20 GeV, neutrino pT > 25 GeV and mT > 40 GeV. The data points (shown with error bars including the statistical and systematic uncertainties) are compared to NLO Monte Carlo predictions with different PDF sets. The PDF uncertainty bands include experimental uncertainties as well as model and parametrization uncertainties.

Summary of W/Z cross section results

-comparison between theory and CMS measurements-

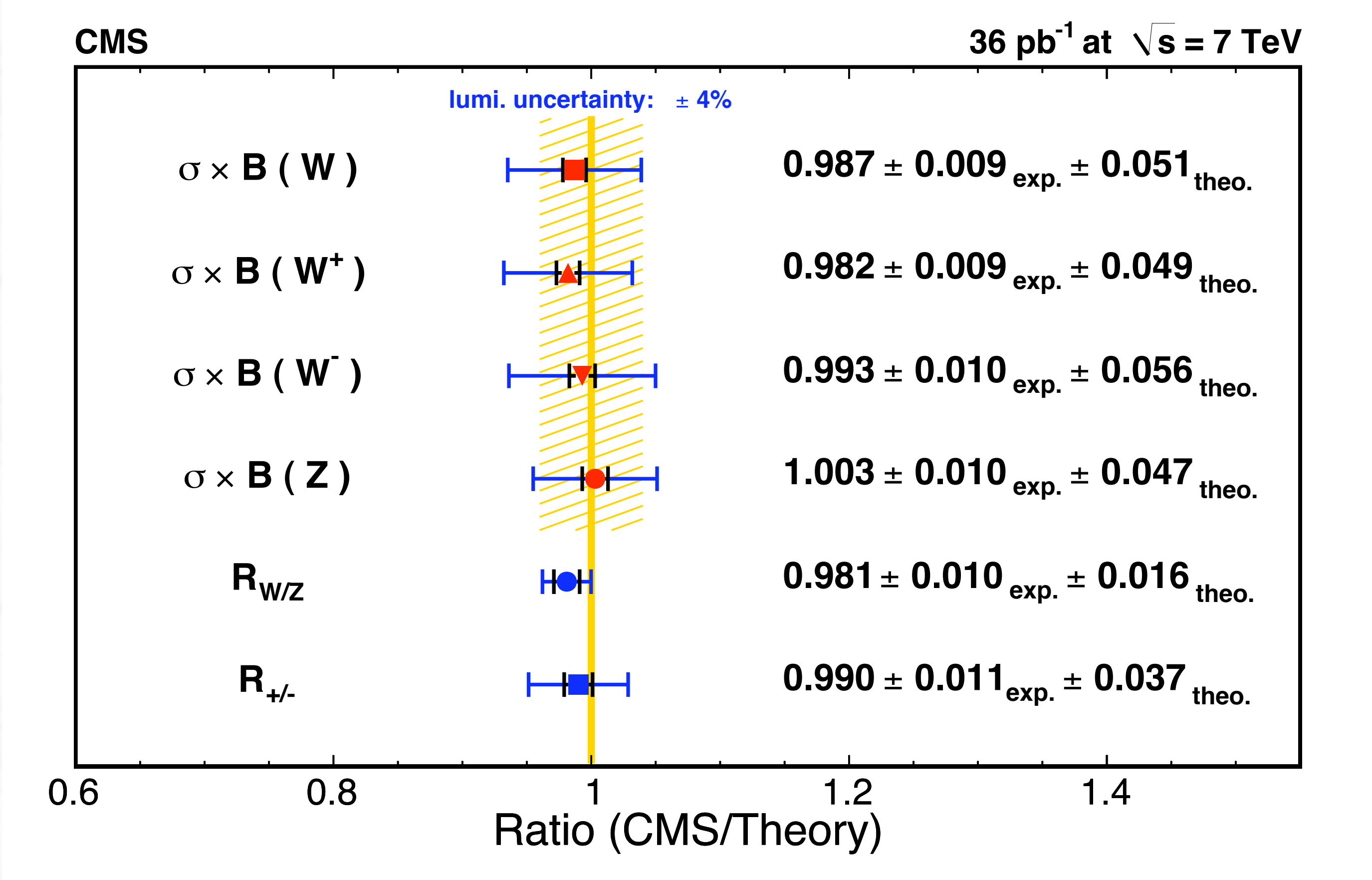

Good agreement between data and NNLO QCD predictions for all measurements

Test of QCD in W/Z + jet production

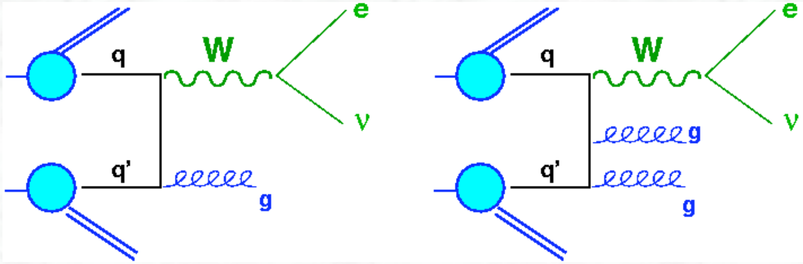

- LO predictions fail to describe the data;
- Jet multiplicities and p_T spectra in agreement with NLO predictions within errors; NLO central value ~10% low

Jet multiplicities in Z+jet production

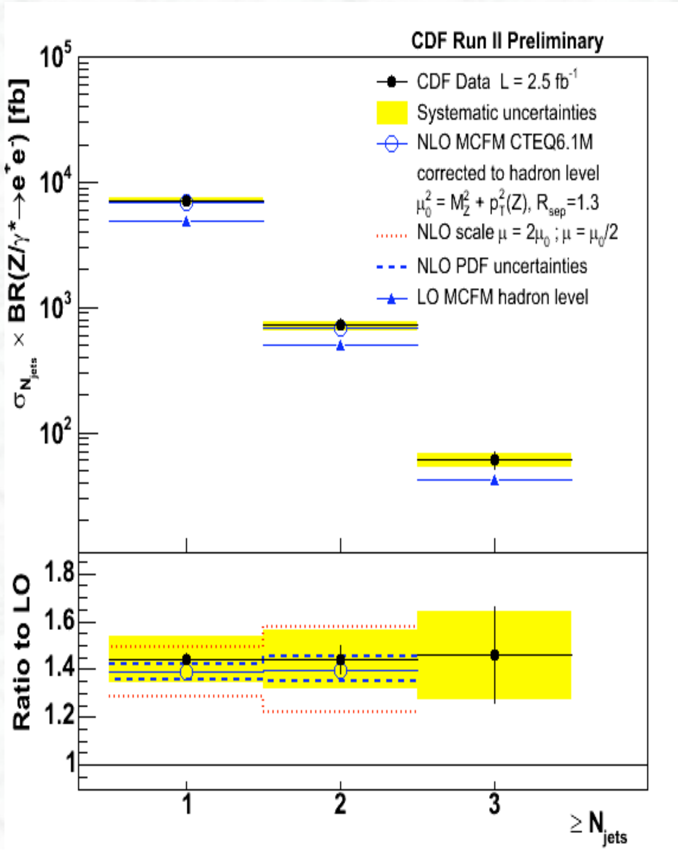

p_T spectrum of leading jet

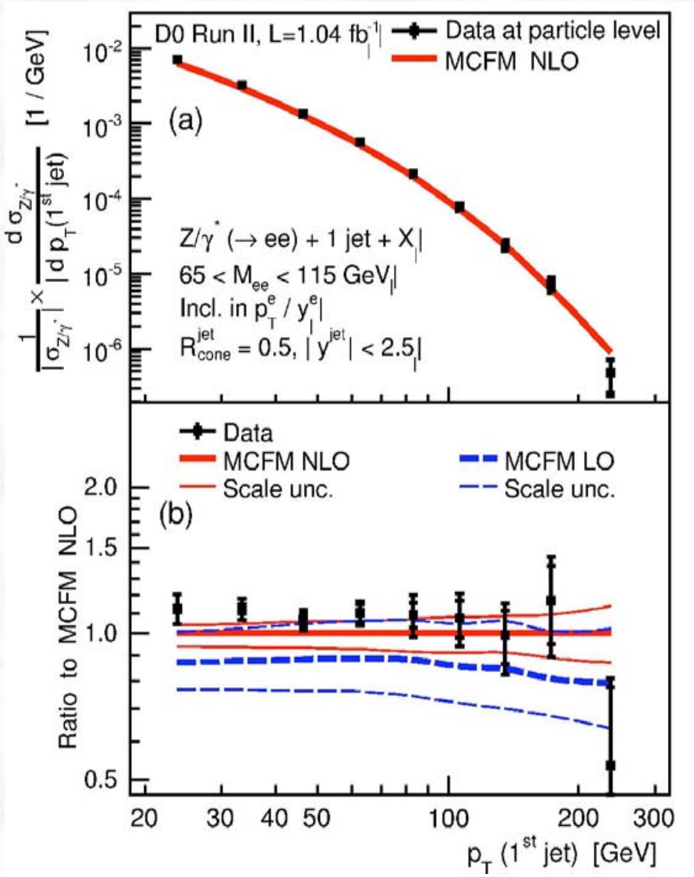

Measurements of W+jets in ATLAS

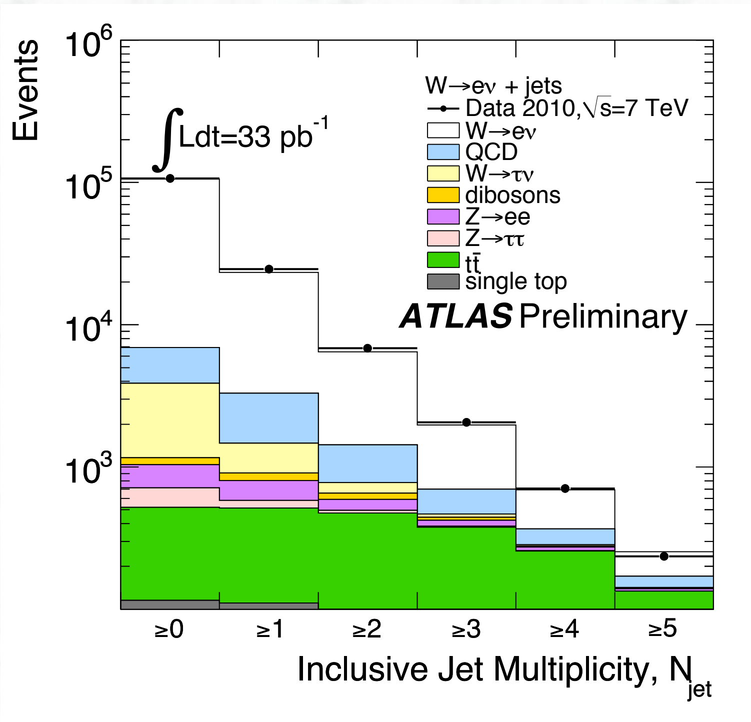

The uncorrected inclusive jet multiplicity distribution for electron channel. The signal and leptonic backgrounds are normalised to the NNLO cross sections. The jet background from QCD processes was determined from data.

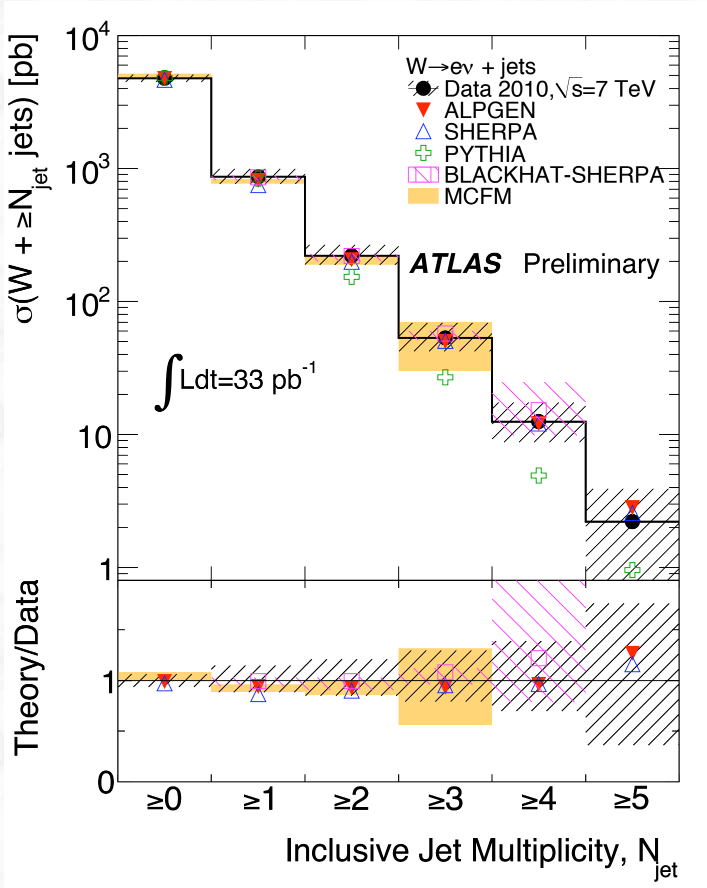

W+jets fiducial cross section results as a function of corrected jet multiplicity for the e channel. The combined statistical and systematic uncertainties are shown by the black-hashed regions. Also shown are predictions from ALPGEN, SHERPA, PYTHIA, MCFM and BLACKHAT-SHERPA, and the ratio of theoretical predictions to data. The theoretical uncertainties are shown only for MCFM (NLO prediction for Njet < 2 and a LO prediction for Njet= 3) and BLACKHAT-SHERPA (NLO prediction for Njet < 3 and a LO prediction for Njet = 4).

p_T spectra of the associated jets

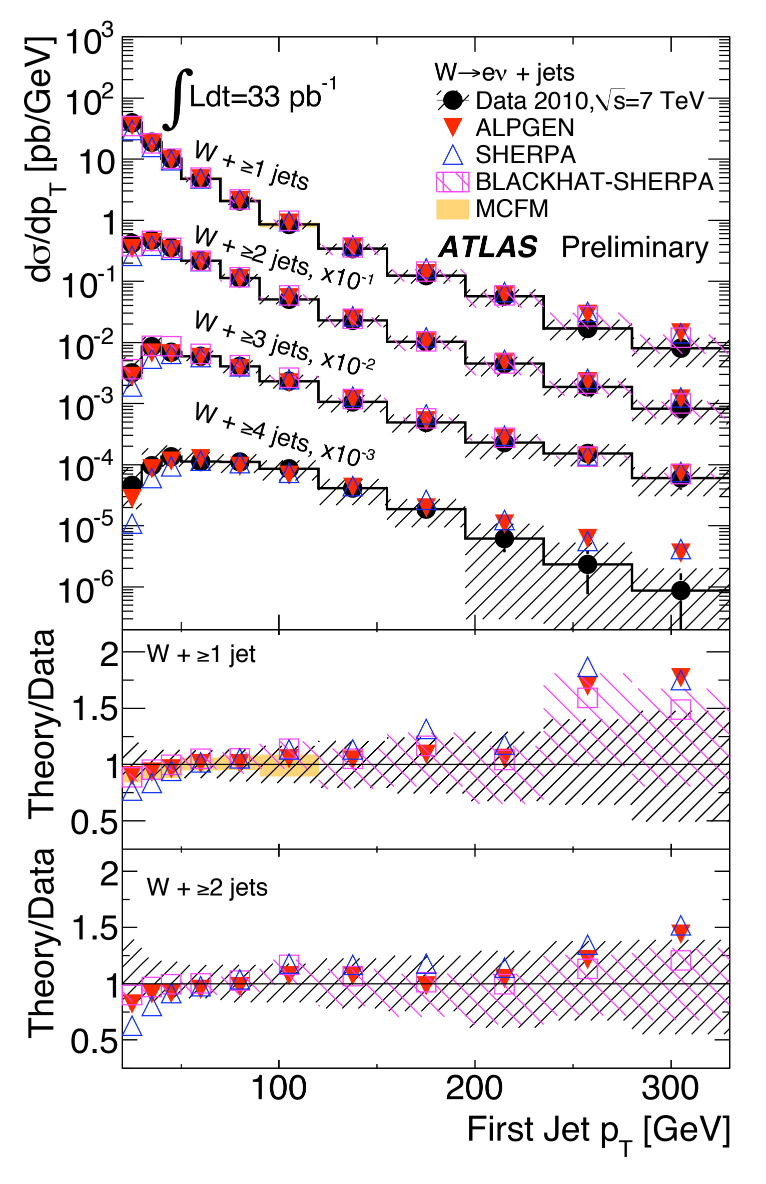

W+jets fiducial cross section (e channel) as a function of the p_T of the first jet in the event. The p_T of the first jet is shown separately for events with >=1 jet to >=4 jet. The >=2 jet, >=3 jet and >= 4 jet distributions have been scaled down by factors of 10 and 100, 1000 respectively. For the data, the combined statistical and systematic uncertainties are shown by the black-hashed regions. Also shown are predictions from ALPGEN, SHERPA, MCFM and BLACKHAT-SHERPA, and the ratio of theoretical predictions to data for >=1 jet to >=2 jet events. The theoretical uncertainties are shown only for MCFM (NLO prediction for Njet < 2 and a LO prediction for Njet= 3) and BLACKHAT-SHERPA (NLO prediction for Njet < 3 and a LO prediction for Njet = 4).

p_T spectra of the associated jets

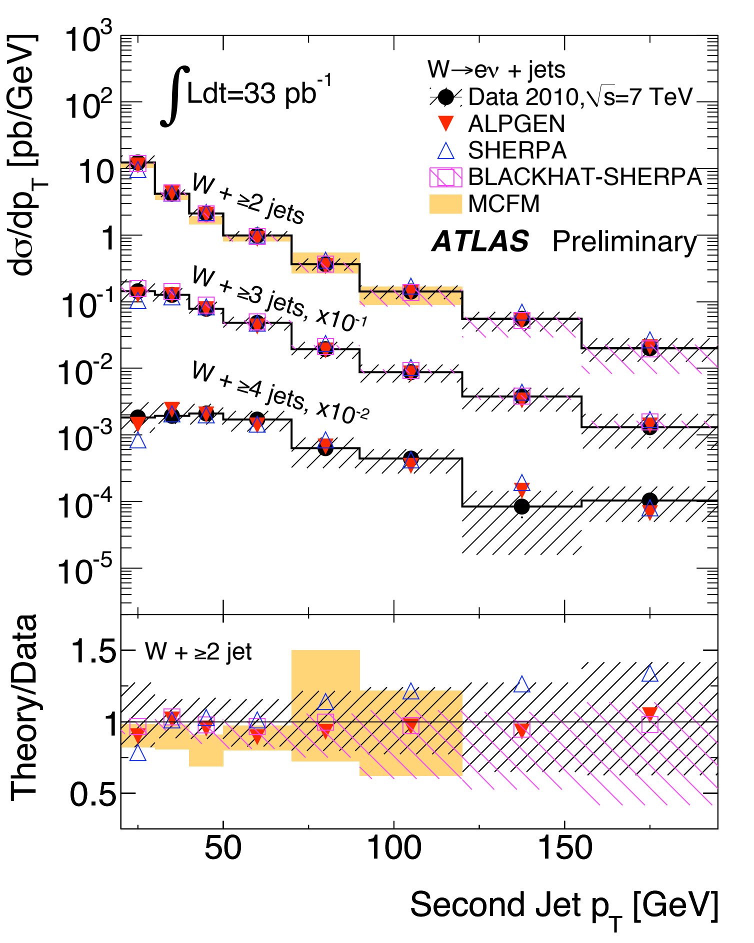

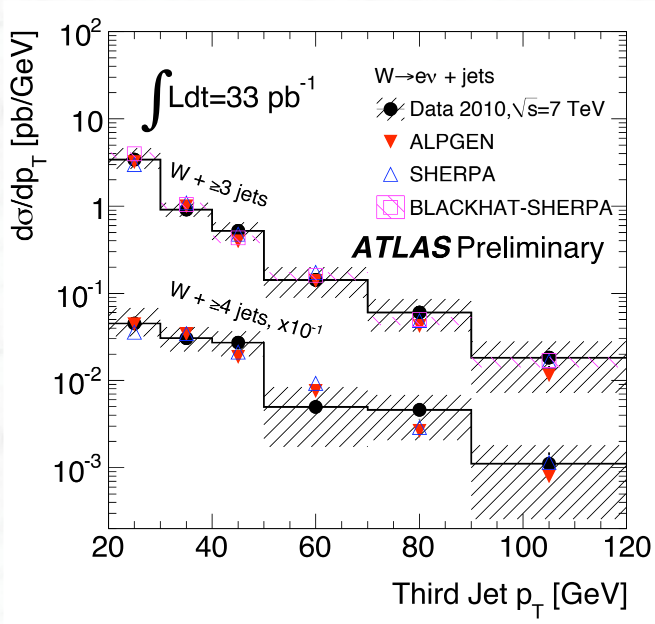

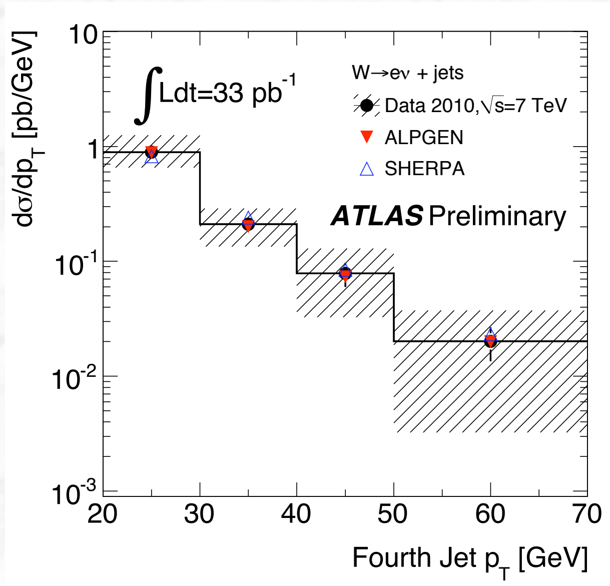

W+jets fiducial cross section (e channel) as a function of the p_T of the second, third and fourth jet in the event.
(further description as above)

Both jet rates and p_T spectra are well described by perturbative QCD calculations

6.5 W mass measurement

Major contributions: LEP-II, direct mass reconstruction

Hadron collider: Tevatron and LHC (in the future)

Precision measurements of m_W and m_{top}

Motivation:

W mass and top quark mass are fundamental parameters of the Standard Model;
The standard theory provides well defined relations between m_W, m_{top} and m_H

Electromagnetic constant
measured in atomic transitions,
e^+e^- machines, etc.

$$m_W = \left(\frac{\pi \alpha_{EM}}{\sqrt{2} G_F} \right)^{1/2} \frac{1}{\sin\theta_W \sqrt{1-\Delta r}}$$

Fermi constant
measured in muon
decay

weak mixing angle
measured at
LEP/SLC

radiative corrections
$\Delta r \sim f(m_{top}^2, \log m_H)$
$\Delta r \approx 3\%$

G_F, α_{EM}, $\sin\theta_W$

are known with high precision

Precise measurements of the W mass and the top-quark mass constrain the Higgs-boson mass
(and/or the theory,
radiative corrections)

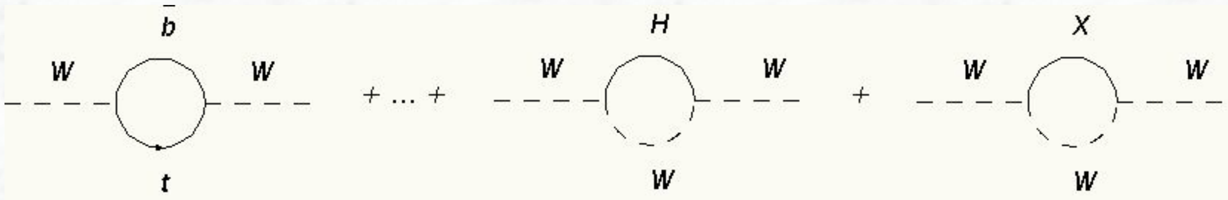

Relation between m_W, m_t, and m_H

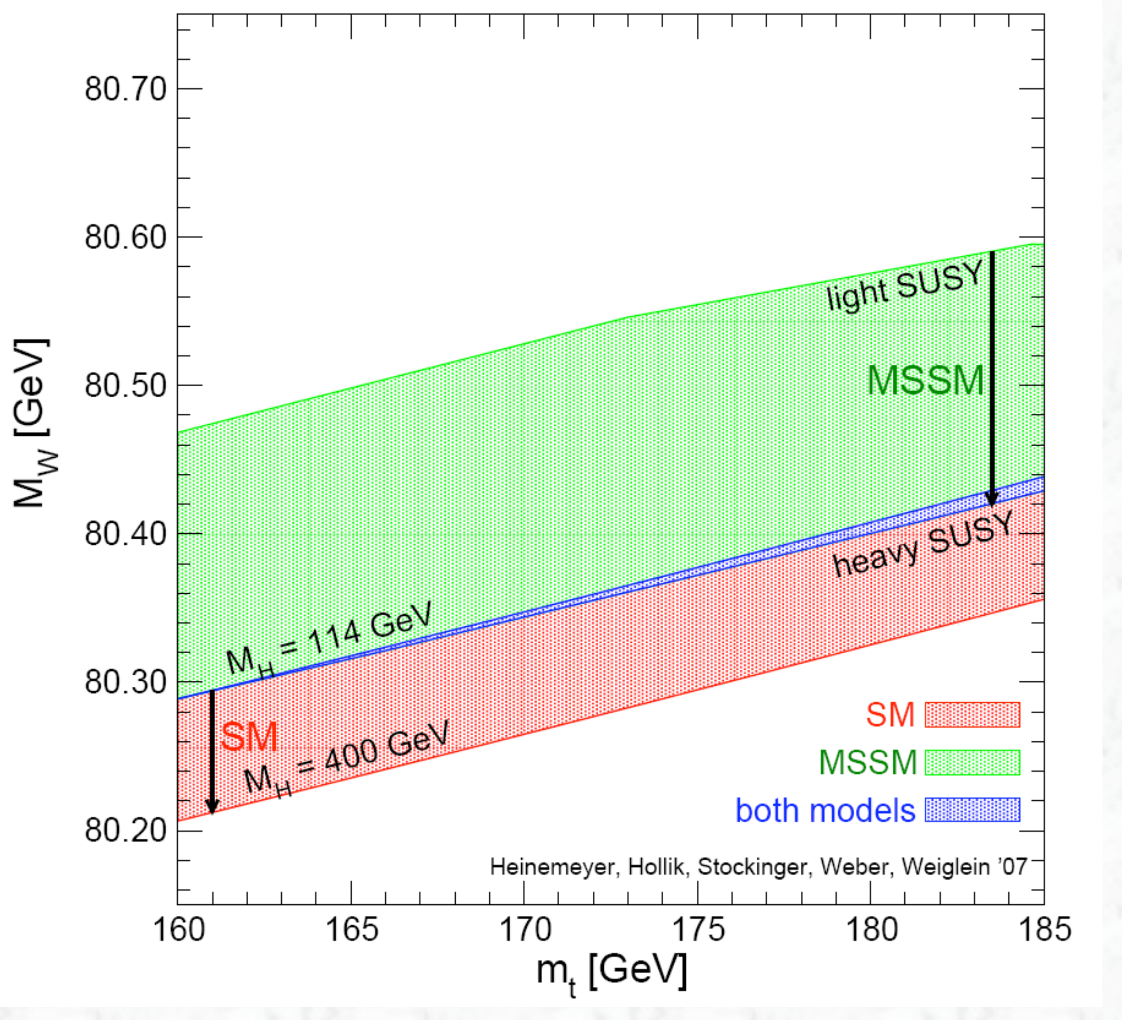

W bosons at LEP – II

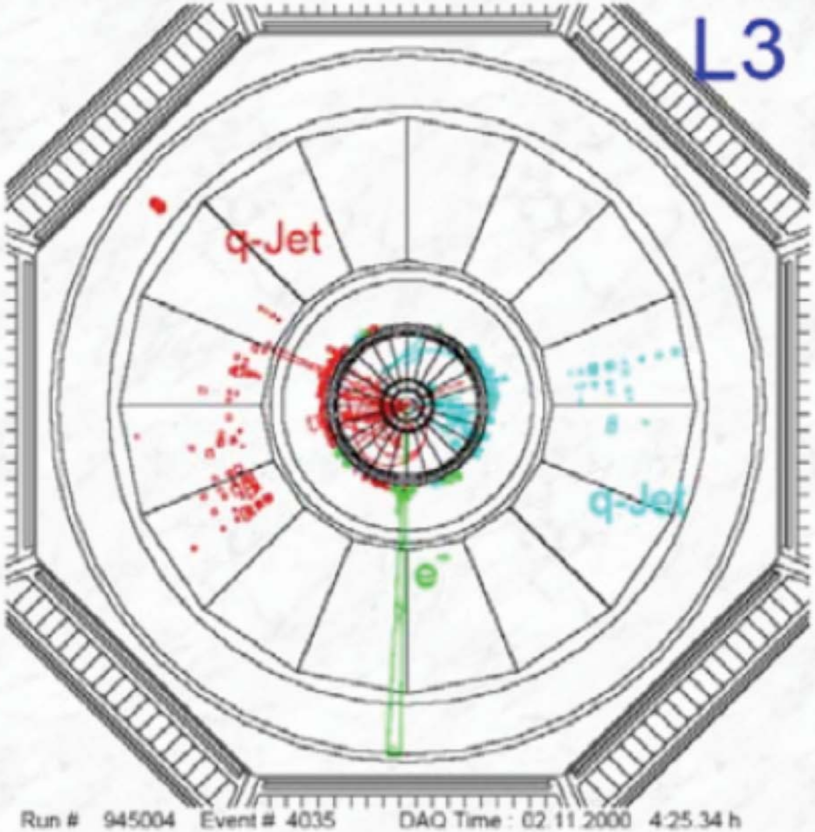

$$WW \to \begin{cases} qq\ell\nu & 44\% \\ qqqq & 45\% \\ \ell\nu\ell\nu & 11\% \end{cases}$$

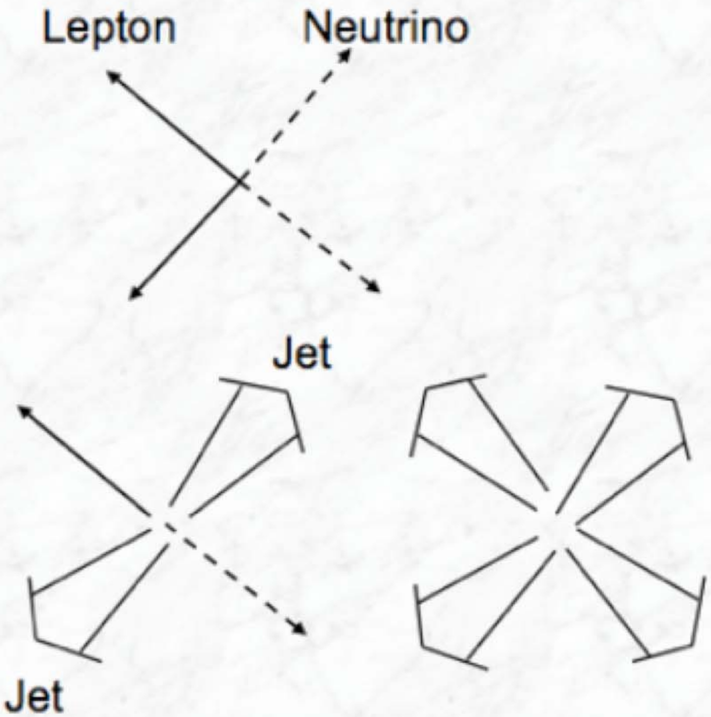

W mass measurement

(1) Messung des WQs an der WW-Produktionsschwelle

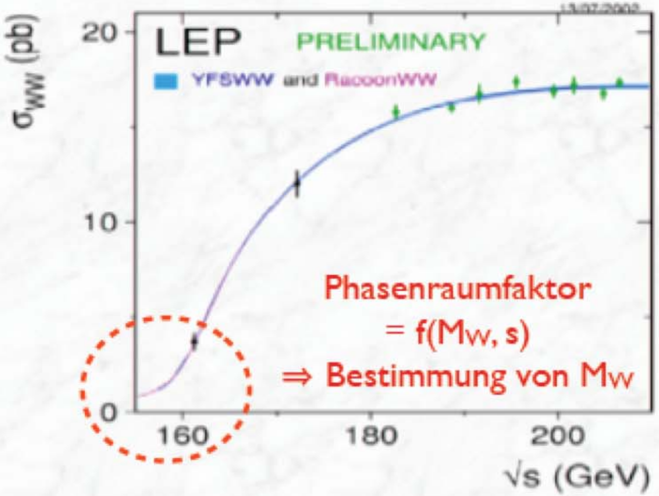

(2) LEP-II: Direkte Rekonstruktion der invarianten Masse des W-Bosons:

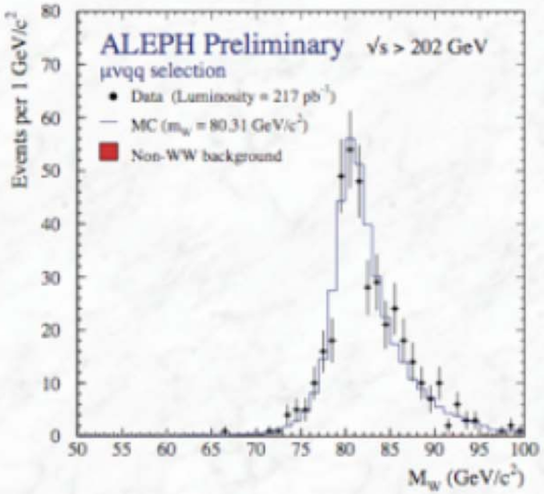

Results from W mass measurements at LEP-II

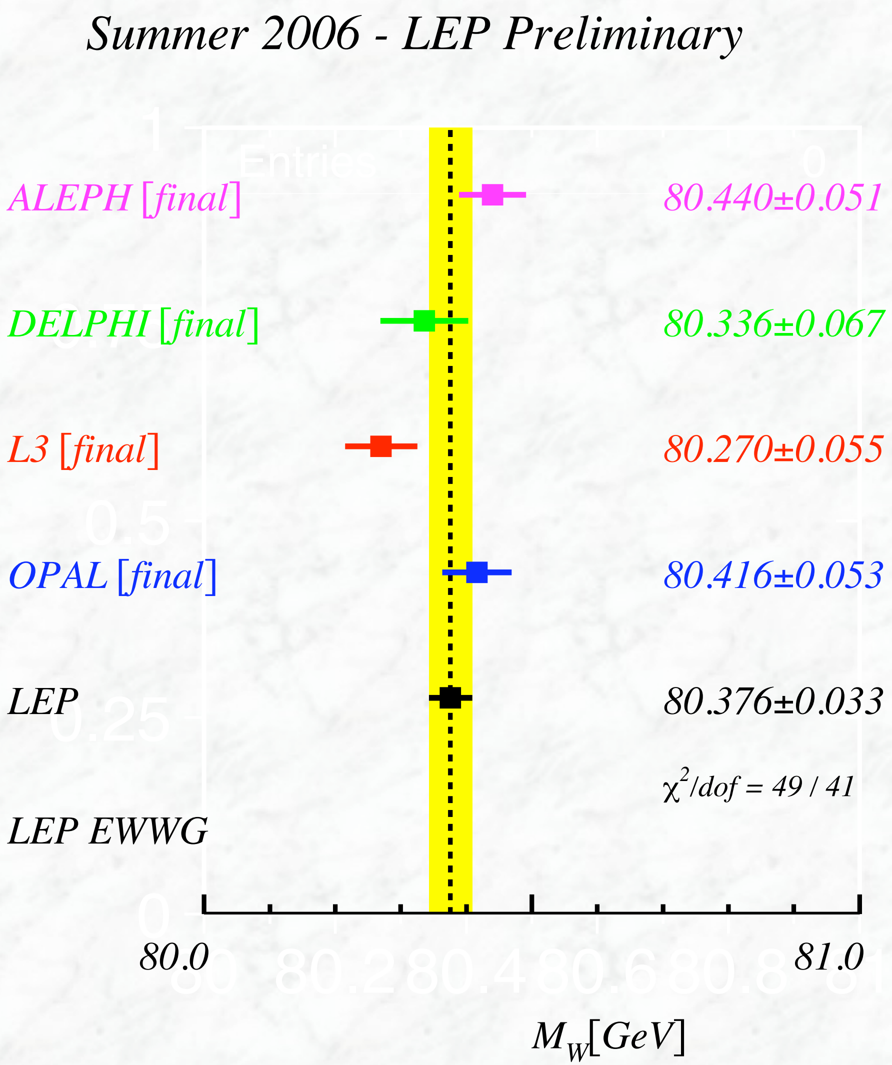

- Results from all four LEP experiments are consistent
- Statistical error is dominant
- Total precision from LEP-II

  $\Delta m_W = \pm 33$ MeV

Results of electroweak precision tests at LEP (cont.)

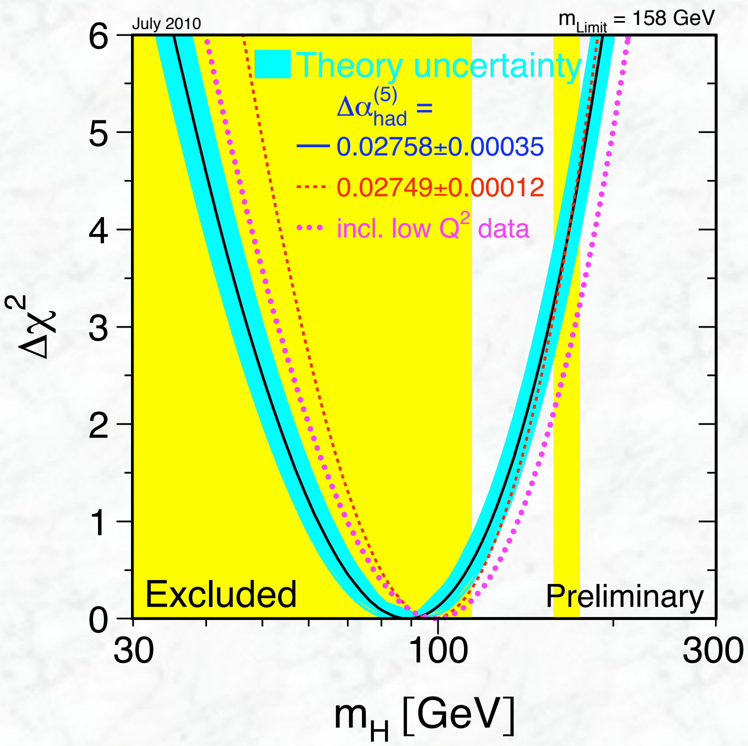

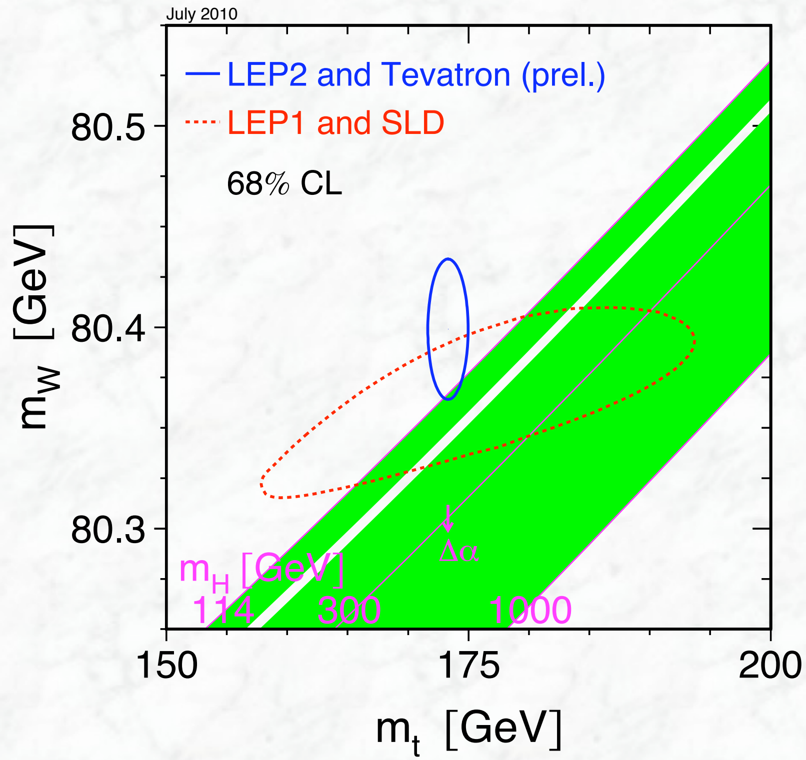

- Radiative corrections (loop, quantum corrections) can be used to constrain yet unobserved particles (however, sensitivity to m_H only through log terms)
- Main reason for continued precision improvements in m_t , m_W

Correlation between m_H and m_W

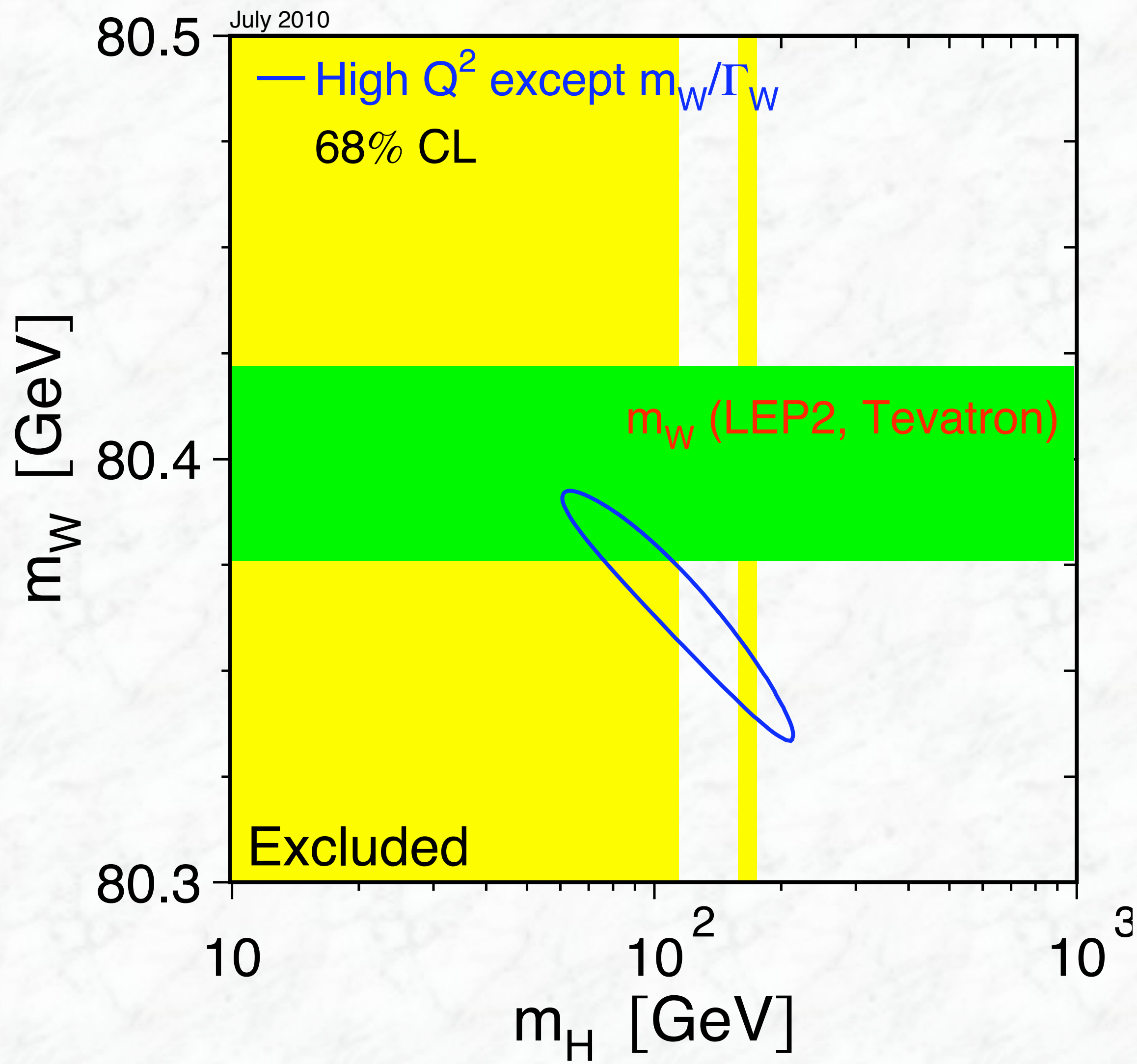

What can hadron collider contribute ?

How can W mass be measured in hadronic collisions ?

Technique used for W mass measurement at hadron colliders:

Event topology:

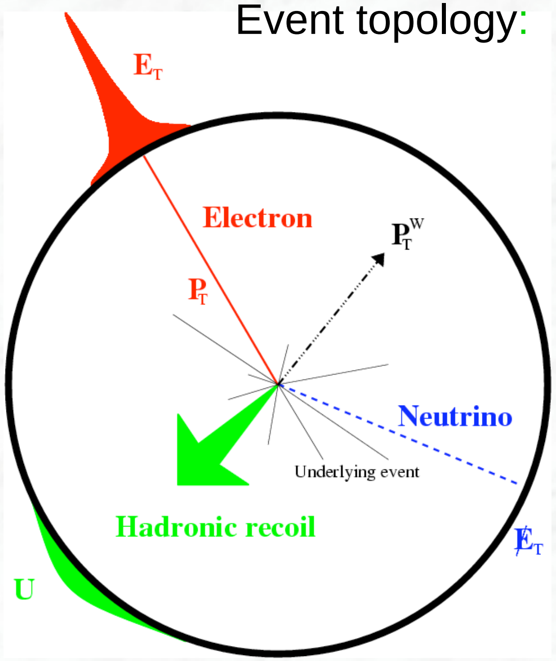

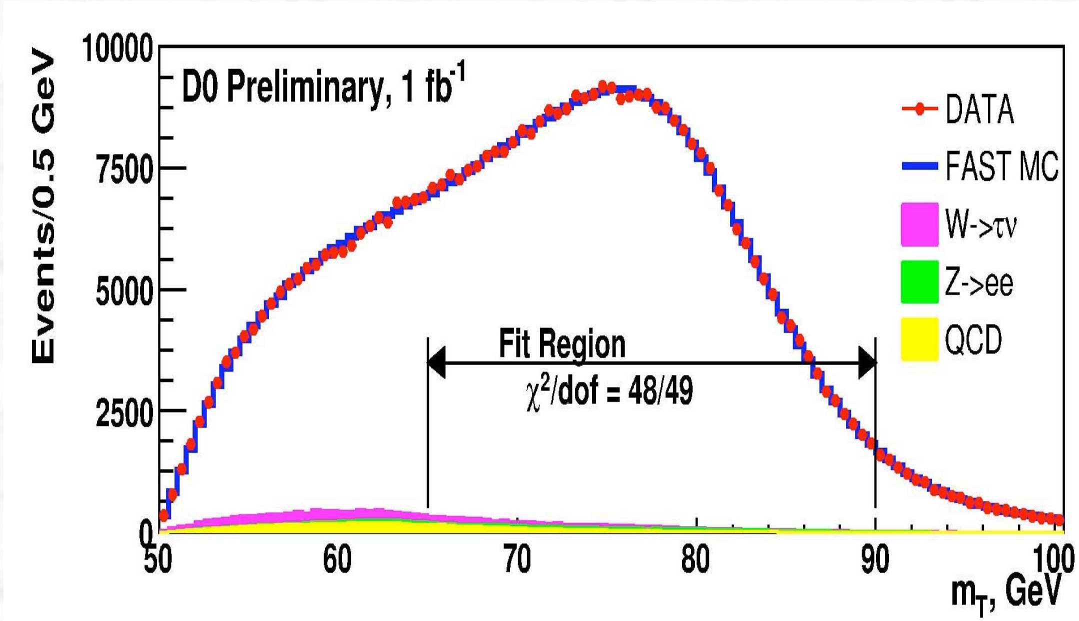

Observables: $P_T(e)$, $P_T(had)$

$\Rightarrow$ $P_T(\nu)$ = - ($P_T(e)$ + $P_T(had)$) long. component cannot be measured

$$\Rightarrow \quad M_W^T = \sqrt{2 \cdot P_T^l \cdot P_T^\nu \cdot \left(1 - \cos\Delta\phi^{l,\nu}\right)}$$

In general the transverse mass M_T is used for the determination of the W mass (smallest systematic uncertainty).

Shape of the transverse mass distribution is sensitive to m_W, the measured distribution is fitted with Monte Carlo predictions, where m_W is a parameter

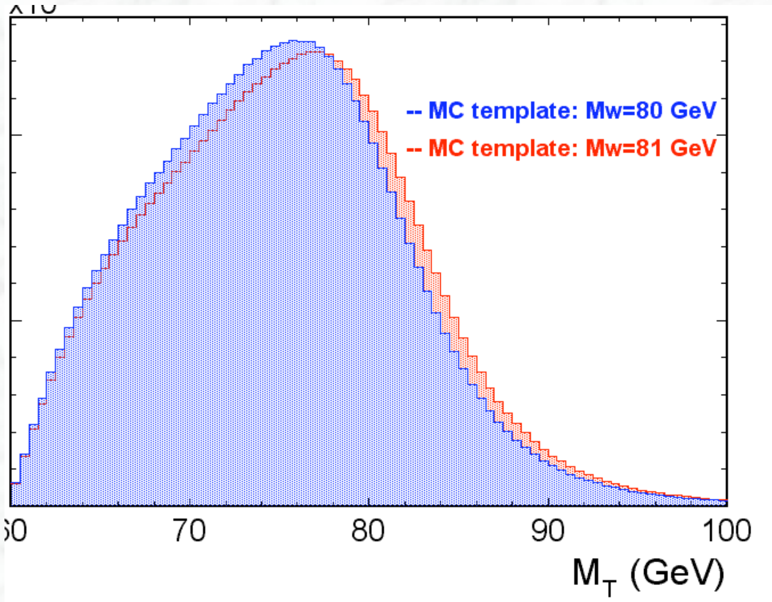

Main uncertainties:

Ability of the Monte Carlo to reproduce real life:

- Detector performance
  (energy resolution, energy scale, ...)
- Physics: production model
  $p_T(W)$, Γ_W, ...
- Backgrounds

In principle any distribution that is sensitive to m_W can be used for the measurement;

Systematic uncertainties are different for the various observables.

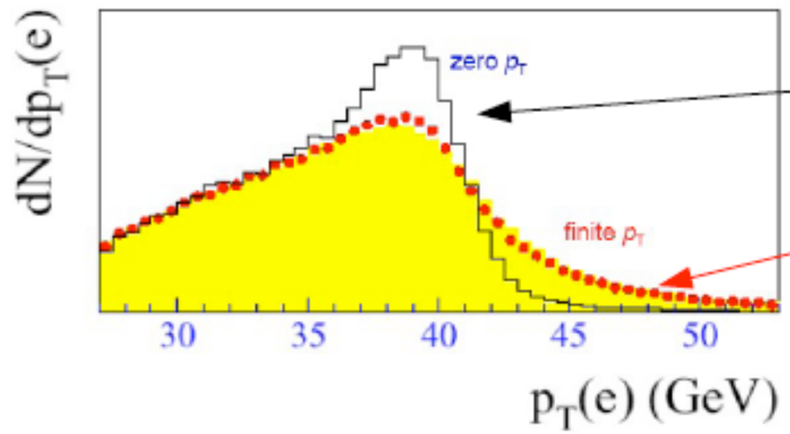

True distribution

Including $p_T(W)$ effects

Including detector effects

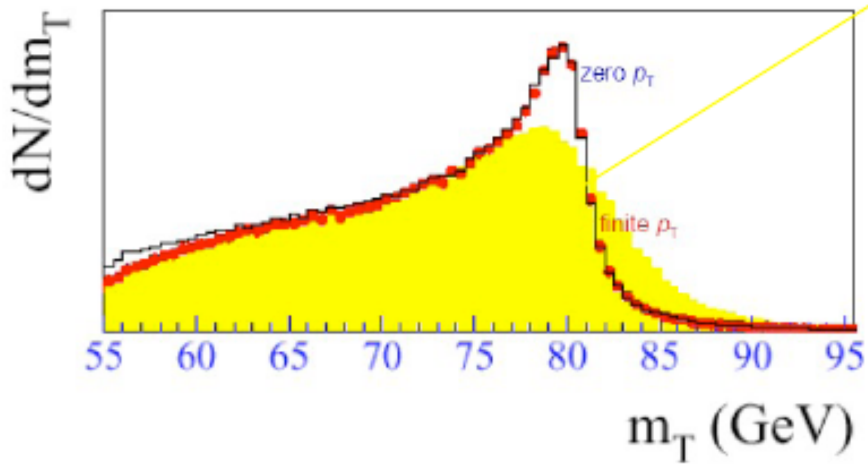

$p_T(e)$ not sensitive to detector effects, requires $p_T(W)$ knowledge

Transverse mass less sensitive to $p_T(W)$, requires good modeling of missing E_T

What precision can be reached in Run II and at the LHC ?

Numbers for a single decay channel

$W \rightarrow e\nu$

Int. Luminosity	CDF 0.2 fb^{-1}	DØ 1 fb^{-1}	LHC 10 fb^{-1}
Stat. error	**48 MeV**	**23 MeV**	**2 MeV**
Energy scale, lepton res.	30 MeV	34 MeV	4 MeV
Monte Carlo model (P_T^W, structure functions, photon-radiation….)	16 MeV	12 MeV	7 MeV
Background	8 MeV	2 MeV	2 MeV
Tot. Syst. error	**39 MeV**	**37 MeV**	**8 MeV**
Total error	**62 MeV**	**44 MeV**	**~10 MeV**

- Tevatron numbers are based on real data analyses
- LHC numbers should be considered as „ambitious goal“
  - Many systematic uncertainties can be controlled in situ, using the large $Z \rightarrow \ell\ell$ sample ($p_T(W)$, recoil model, resolution)
  - Lepton energy scale of ± 0.02% has to be achieved to reach the quoted numbers

Combining both experiments (ATLAS + CMS, 10 fb^{-1}), both lepton species and assuming a scale uncertainty of ± 0.02% a total error in the order of

⇒ Δm_W ~ ± 10 - 15 MeV might be reached.

Signature of Z and W decays

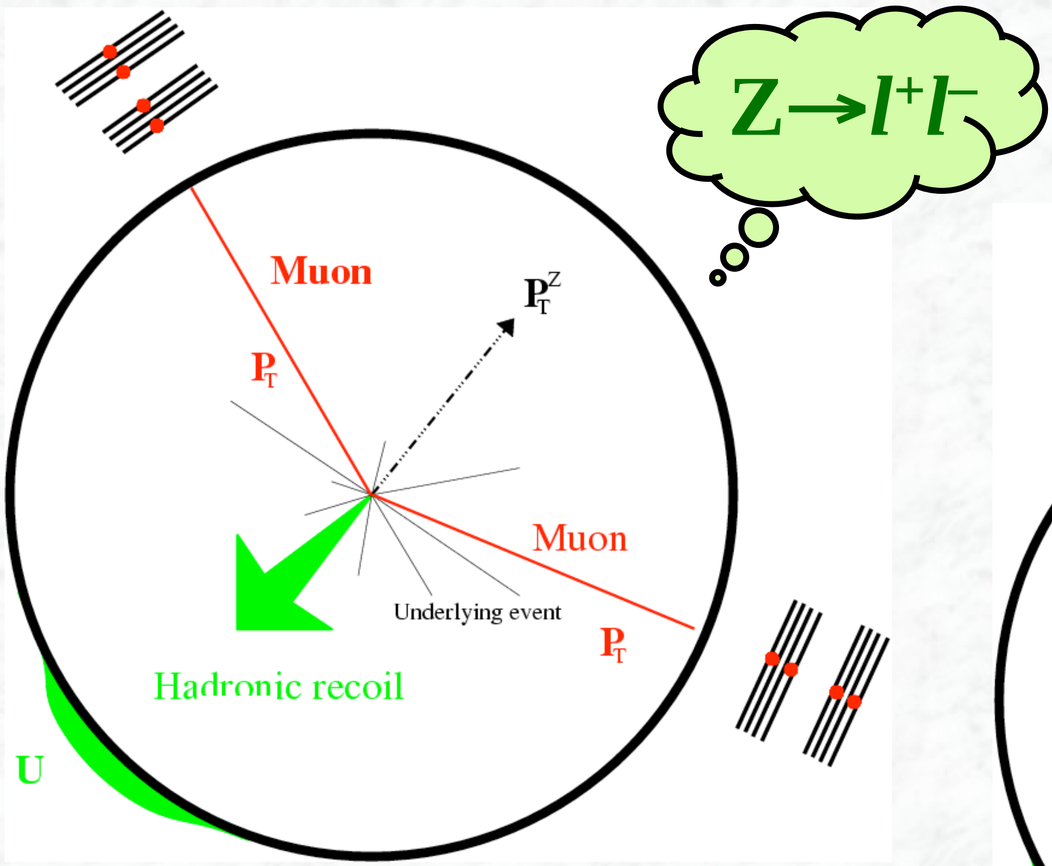

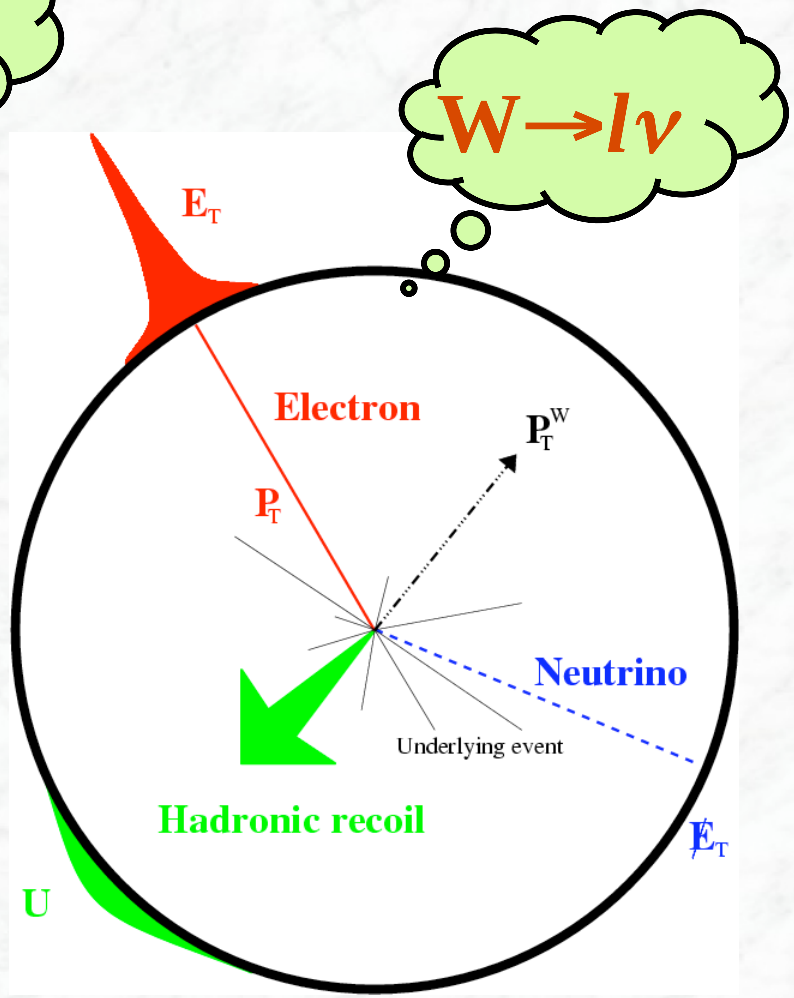

What precision can be reached in Run II and at the LHC ?

Numbers for a single decay channel

$W \to e\nu$

Int. Luminosity	CDF 0.2 fb^{-1}	DØ 1 fb^{-1}	LHC 10 fb^{-1}
Stat. error	**48 MeV**	**23 MeV**	**2 MeV**
Energy scale, lepton res.	30 MeV	34 MeV	4 MeV
Monte Carlo model (P_T^W, structure functions, photon-radiation….)	16 MeV	12 MeV	7 MeV
Background	8 MeV	2 MeV	2 MeV
Tot. Syst. error	**39 MeV**	**37 MeV**	**8 MeV**
Total error	**62 MeV**	**44 MeV**	**~10 MeV**

- Tevatron numbers are based on real data analyses
- LHC numbers should be considered as „ambitious goal“
  - Many systematic uncertainties can be controlled in situ, using the large $Z \to \ell\ell$ sample (PT(W), recoil model, resolution)
  - Lepton energy scale of ± 0.02% has to be achieved to reach the quoted numbers

Combining both experiments (ATLAS + CMS, 10 fb^{-1}), both lepton species and assuming a scale uncertainty of ± 0.02% a total error in the order of

$\Rightarrow$ $\Delta m_W \sim \pm$ 10 - 15 MeV might be reached.

Summary of W-mass measurements

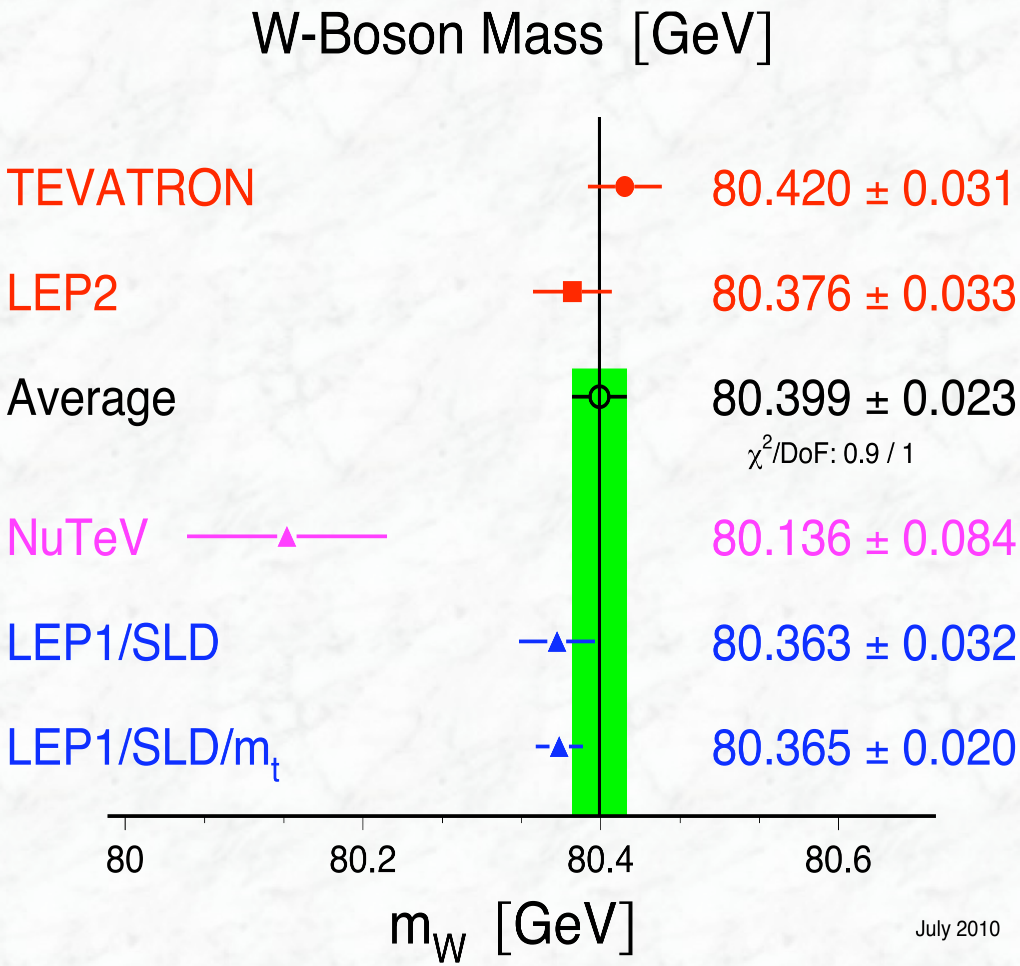

Precison obtained at the Tevatron is superior to the LEP-II precision

Further improvements are expected from LHC (may take some time, pile-up makes the measurement very challenging)

m_W (from LEP2 + Tevatron) = 80.399 ± 0.023 GeV

$3 \cdot 10^{-4}$